IEEE Access
Multidisciplinary | Rapid Review | Open Access Journal

Received November 18, 2021, accepted December 6, 2021, date of publication December 10, 2021,
date of current version December 23, 2021.

Digital Object Identifier 10.1109/ACCESS.2021.3134872

Reconfiguration of Distribution Networks With Distributed Generations Using an Improved Neural Network Algorithm

THANH VAN TRAN[1], BAO-HUY TRUONG[1], TRI PHUOC NGUYEN[2], THI ANH NGUYEN[2], THANH LONG DUONG[3], AND DIEU NGOC VO[2,4]

[1]Institute of Engineering and Technology, Thu Dau Mot University (TDMU), Thu Dau Mot, Binh Duong 75109, Vietnam
[2]Department of Power Systems, Ho Chi Minh City University of Technology (HCMUT), Ho Chi Minh City 72506, Vietnam
[3]Faculty of Electrical and Electronic Technology Engineering, Industrial University of Ho Chi Minh City, Ho Chi Minh City 71408, Vietnam
[4]Vietnam National University Ho Chi Minh City (VNU-HCM), Linh Trung Ward, Thu Duc, Ho Chi Minh City 71308, Vietnam

Corresponding author: Dieu Ngoc Vo (vndieu@hcmut.edu.vn)

This work was supported by Thu Dau Mot University (TDMU) under Grant DT.21.1-079.

ABSTRACT This study aims to suggest a new quasi-oppositional chaotic neural network algorithm (QOCNNA) for simultaneous network reconfiguration and distributed generations allocation (SNR-DG) in radial distribution networks (RDNs). The proposed QOCNNA is developed by combining original NNA with chaotic local search (CLS) and quasi-oppositional-based learning (QOBL) approaches. Integration of QOBL helps the algorithm improve exploration of the search space and convergence speed. Meanwhile, CLS can improve exploitation of the algorithm by performing local search around the current best solution. The objective of the SNR-DG problem is to define the network configuration, settings of distributed generations to optimize active power loss and voltage stability in RDNs. The performance of QOCNNA is tested on the SNR-DG problem with 33-, 69- and 118-bus RDNs considering different scenarios. The result analysis indicates that SNR-DG implementation is effective for power loss reduction and voltage stability improvement. Notably, QOCNNA yields active power loss reductions and voltage stability index improvements associated with case multi-objective SNR-DG at nominal load condition of {70.79%, 16.36%}, {84.02%, 8.59%}, and {57.79%, 10.10%}, respectively, for 33-, 69-, and 118-bus RDNs. In comparison with previous studies, QOCNNA is more effective in improving the performance of RDNs. Compared with other methods that we have applied, QOCNNA dominates the performance in solution accuracy, convergence speed, and robustness for all case studies. Also, QOCNNA finds effective and feasible solutions for daily variable load and generation scenario with the minimized total annual energy loss. Simulated outcomes in this scenario verify the superiority of QOCNNA over analytical-based approaches and the applied methods regarding total annual energy loss reduction and cost savings as well. There are hence simulation-based evidences to state that the CLS and QOBL help QOCNNA achieve a good trade-off between exploration and exploitation. Thus, QOCNNA has proved to be a favorable method in dealing with the SNR-DG problem.

INDEX TERMS Distributed generations, neural network algorithm, network reconfiguration, radial distribution networks.

I. INTRODUCTION

Radial distribution network (RDN) plays a crucial role in the power systems, responsible for power supply from the transmission systems to the customer. However, the continuously growing load has posed challenges for power companies to operate RDN efficiently and reliably. Power loss significantly affects the operating efficiency of RDNs. Hence, it is imperative to reduce power loss for RDNs to operate efficiently and economically. In this regard, many approaches have been implemented to minimize the power losses of RDNs. Network reconfiguration (NR) and distributed generation (DG) integration are two prominent techniques that attract much attention due to the development context of power sources

The associate editor coordinating the review of this manuscript and approving it for publication was Emanuele Crisostomi.

and investment costs. NR is an effective method to minimize power loss in RDNs. RDNs are operated in the radial topology to decrease the fault level and protect coordination effectively. Tie-line switches (normally opened) and sectionalizing switches (normally closed) are two types of switches in RDNs. NR leads to a new network topology by altering the opened/closed status of switches while maintaining the radial topology of the system. NR is a vital grid strategy that decreases active power losses, improves voltage profile and system reliability [1]. Moreover, NR can transfer load from one branch to another to avoid overloading. Recently, distributed generations (DGs) have been swiftly integrated into RDNs due to electricity deregulation, fossil fuel depletion, and environmental concerns. Apart from NR implementation, the deployment of DG units is also a well-known grid strategy to decrease power losses and boost the voltage profile of RDNs. Therefore, the NR application in RDNs should be studied in the presence of DGs.

Since the NR problem was firstly introduced by Merlin and Back [2], a large amount of research has also been done on the NR problem using various approaches from heuristic approaches like branch-and-bound method [2], modified branch exchange method [3], and switch exchange method [4] to metaheuristic approaches like particle swarm optimization (PSO) [5], [6], genetic algorithm (GA) [7], biased random key GA (BRKGA) [8], harmony search algorithm (HSA) [9], heuristic rules-based fuzzy multiple objectives [10], fireworks algorithm (FWA) [11], GA with varying population (GAVP) [12], and cuckoo search algorithm (CSA) [13]. In general, heuristic methods are characterized by fast convergence, but they lack the ability to handle large-scale systems with many constraints. Meanwhile, metaheuristic methods have robust searchability to discover optimal solutions or near-optimal solutions, which are well suited for large-scale networks. Hence, the applications of metaheuristic methods to NR problems are constantly evolving. Recently, many researchers have applied several artificial intelligence and analytical methods to solve the optimal DGs allocation problem in RDNs. In [14], comprehensive analytical expressions were suggested to define the allocation of PV units for maximizing the technical benefits in RDN. The objective functions include active and reactive power losses, voltage stability index, line congestion margin and voltage deviations. Mahmoud and Lehtonen [15] proposed generic closed-form analytical expressions to determine optimal locations and sizes of multi-type DGs and capacitors for optimizing reactive power loss in RDNs. Moreover, the proposed method incorporated an optimal power flow (OPF) algorithm to consider the constraints of systems. In [16], the authors utilized an efficient analytical (EA) method to obtain an optimal mix of different DG types with various generation capabilities to minimize power losses in RDNs.

Researchers have constantly proposed new methods to achieve better performance for RDNs. One of those efforts is the simultaneous integration of NR and optimal DGs placement. Recent studies on the integration of these two effective strategies have been done using metaheuristic methods. Shaheen *et al.* [17] developed an improved equilibrium optimization algorithm (IEOA) to deal with the optimal integration of NR with DGs. Different load conditions of 33- and 69-bus systems were utilized to test the IEOA method, and its superiority was confirmed. Onlam *et al.* [18] applied the adaptive shuffled frogs leaping algorithm to acquire optimal NR and DGs settings on several circumstances of 33- and 69-bus RDNs to minimize system losses and enhance voltage profile. Murty and Kumar [19] suggested NR and optimal renewable-based DGs placement considering load uncertainties. A hybrid fuzzy-bees approach was developed by Tolabi *et al.* [20] for NR with DG placement for reducing power losses, improving the feeder load balancing and voltage profile. In [21], an artificial bee colony was combined with a hybrid method of HSA and PSO to deal with the combined problem of NR with shunt capacitors and DGs allocation to optimize the power loss. In [22], a fuzzy multi-objective technique was utilized for handling NR. Afterwards, a heuristic approach was applied to obtain the optimal NR, which generated a solution based on the initial NR. In [23], an improved plant growth simulation method was proposed for NR with DGs presence for power loss reduction. Optimal DG locations were defined using sensitivity analysis. Bayat *et al.* [24] developed a heuristic approach for NR and DGs allocation to maximize loss reduction. In [25], levy flights embedded in sine–cosine algorithm to deal with NR and DGs allocation in 33-bus and 69-bus RDNs. The proposed problem considered power losses and voltage stability index objectives. Some other typical metaheuristic methods have also been applied to handle the combination of NR and DGs allocation, such as HSA [26], adaptive CSA [27], FWA [28], big-bang crunch algorithm [29], [30], hybrid grey wolf optimizer and PSO (GWO-PSO) [31], electromagnetism-like mechanism (ELM) [32], firefly (FF) [33], and three-dimensional group search optimization (3D-GSO) [34].

Based on the aforesaid literature survey, applying the metaheuristic algorithms to the integration of NR with DGs placement has several certain limitations. Most of the previous studies only focused on small- and medium-scale RDNs without considering large-scale RDNs. Moreover, integration of NR and DGs placement is a combined optimization problem, which poses a challenge to achieve optimal solutions due to its complexity. Although the powerful search capabilities of metaheuristic algorithms are well suited for achieving optimal solutions, there is no guarantee that they will be effective for all optimization problems [35]. Such methods may not yield reasonable quality solutions and may get stuck at a local optimum. Therefore, developing an appropriate algorithm is of interest to effectively solve the simultaneous NR and DGs placement, especially for large-scale systems.

Recently, a new meta-heuristic method inspired by biological nervous systems and artificial neural networks (ANNs), namely neural network algorithm (NNA), has been developed by Sadollah *et al.* [36]. Thanks to the ANNs structure, NNA

has proven its high performance for benchmark functions. Furthermore, NNA is a parameter-free metaheuristic method; hence, algorithm parameters do not need to be fine-tune except for the population size and stopping criteria, making NNA easy to implement to solve optimization problems. Nevertheless, NNA has the notable disadvantage of converging prematurely and getting stuck in local minima due to its stochastic nature. Hence, improving the performance of NNA to efficiently solve the simultaneous NR and DGs placement problem is certainly worth further consideration.

Motivated by the above problems, this study proposes a new modified NNA called quasi-oppositional chaotic neural network algorithm (QOCNNA) to deal with the simultaneous NR and DGs integration (SNR-DG) problem in RDNs. The SNR-DG problem aims to minimize active power loss and maximize voltage stability index while sustaining system constraints, including power balance, feeder capacity limits, bus voltage limits, capacity and penetration limits of DGs, and radial topology constraints. QOCNNA was developed by integrating chaotic local search (CLS) and quasi-opposition-based learning (QOBL) strategies into the structure of NNA. QOBL is a highly effective strategy that helps meta-heuristic algorithms improve global search ability to explore more promising regions on the design domain. In addition to QOBL, CLS is a strategy to boost the local search ability of algorithms to exploit promising regions (i.e., neighborhoods of best solutions). The incorporation of QOBL and CLS strategies aims to strike a good equilibrium between the exploration and exploitation tendencies of QOCNNA. The proposed QOCNNA was evaluated on 33-bus small-scale, 69-bus medium-scale, and 118-bus large-scale RDNs with different scenarios at different load conditions. Considering practical situation of daily variable load demand and generation, an effective methodology has been developed to determine the optimal network configuration and settings of DG according to a 24-h load curve and an hourly output curve of photovoltaic (PV) DG so that total annual energy loss is minimized. QOCNNA was compared with the original NNA, ant lion optimizer (ALO), whale optimization algorithm (WOA), sine cosine algorithm (SCA), and different intelligent algorithms in the literature, where its robustness and efficiency in solving the SNR-DG problem was proved.

The contributions of this study are presented as below:

- A new meta-heuristic algorithm, namely QOCNNA, is developed to deal with the SNR-DG problem, where real power loss and voltage stability index are simultaneously optimized.
- The QOCNNA is validated on the 33-bus, 69-bus, and 118-bus RDNs. Different scenarios at three load conditions are also investigated for the SNR-DG problem.
- The performance of RDNs is remarkably enhanced in terms of active power loss, voltage profile, and voltage stability after SNR-DG implementation using QOCNNA.
- A new effective methodology is developed to find the optimal network configuration and settings of a PV DG relative to daily variable load and generation scenario to minimize total yearly energy loss. Simulation results from QOCNNA are compared with NNA, ALO [37], WOA [38], SCA [39], and analytical-based methods [40] to demonstrate its effectiveness in this scenario.
- The comparisons of QOCNNA and other algorithms show that QOCNNA obtains better solution quality, convergence speed, and standard deviation of solutions in most case studies.

Section 2 defines the SNR-DG formulation. Then, the QOCNNA concept and its implementation for the SNR-DG problem are introduced in Sections 3 and 4, followed by the simulation results in Section 5. Lastly, Section 6 is the conclusion of this study.

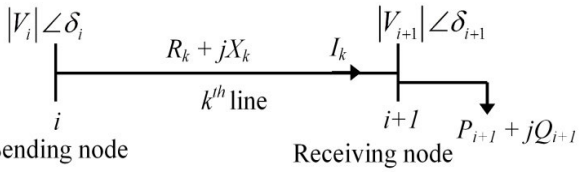

FIGURE 1. A single line of an RDN.

II. PROBLEM FORMULATION

The aim of the SNR-DG problem is to define optimal network configuration, locations and sizes of DGs for minimizing active power loss and maximizing voltage stability index in RDNs while sustaining all operational constraints, which can be generally determined as follows:

A. ACTIVE POWER LOSS

Active power loss in an RDN can be determined as follows:

$$OF_1 = \text{Min}(P_L) = \text{Min}\left(\sum_{k=1}^{N_L} R_k I_k^2\right) \tag{1}$$

where N_L signifies the total number of branches, P_L is the active power loss, R_k denotes the resistance of the k^{th} branch, and I_k represents the current of the k^{th} branch.

B. OVERALL VOLTAGE STABILITY INDEX

A single line of an RDN is portrayed as in Fig. 1. The voltage stability index (VSI) of the $(i+1)^{\text{th}}$ bus is calculated as follows:

$$VSI_{i+1} = |V_i|^4 - 4(P_{i+1}X_k - Q_{i+1}R_k) - 4(P_{i+1}R_k + Q_{i+1}X_k)\,|V_i|^2 \tag{2}$$

where X_k is the reactance of the k^{th} branch.

The overall voltage stability index (OVSI) of an RDN can be defined as the following equation:

$$OVSI = \sum_{i=2}^{N_B} VSI_i \tag{3}$$

where N_B denotes the total number of buses.

The overall stability of the RDN is improved as the OVSI value increases. Hence, the objective to maximize OVSI can be given as follows:

$$OF_2 = \text{Max}(OVSI) = \text{Min}\left(\frac{1}{OVSI}\right) \tag{4}$$

C. MULTI-OBJECTIVE FUNCTION

In this study, active power loss and OVSI are simultaneously considered in a multi-objective function. The fitness function (FF) of the SNR-DG problem can be formulated as follows:

$$FF = \text{Min}\left(w_1 \frac{P_L}{P_{L,base}} + w_2 \frac{OVSI_{base}}{OVSI}\right) \tag{5}$$

where w_1 and w_2 are penalty coefficients, $P_{L,base}$ and $OVSI_{base}$ are values of active power loss and $OVSI$ in the initial case.

D. SYSTEM CONSTRAINTS

The SNR-DG problem must satisfy the following constraints:

1) *Power balance:* The power balance of RDNs must be balanced according to equations:

$$P_S + \sum_{i=1}^{N_{DG}} P_{DG,i} = \sum_{j=1}^{N_B} P_{D,j} + \sum_{k=1}^{N_L} P_{L,k} \tag{6}$$

$$Q_S + \sum_{i=1}^{N_{DG}} Q_{DG,i} = \sum_{j=1}^{N_B} Q_{D,j} + \sum_{k=1}^{N_L} Q_{L,k} \tag{7}$$

where P_S and Q_S denote the active and reactive power outputs at the slack bus, respectively; $P_{DG,i}$ and $Q_{DG,i}$ symbolize the active and reactive power outputs of the i^{th} DG, respectively; $P_{D,j}$ and $Q_{D,j}$ represent the active and reactive powers at the j^{th} bus, respectively; $P_{L,k}$ and $Q_{L,k}$ designate active and reactive power losses of the k^{th} branch, respectively; and N_{DG} represents the total number of DGs.

2) *Bus voltage and feeder capacity limits:* Limit of bus voltages and feeder capacity must be in the permissible ranges:

$$V_{\min,i} \le V_i \le V_{\max,i}, \quad i = 1, \ldots, N_B \tag{8}$$

$$|I_k| \le \left|I_{\max,k}\right|, \quad k = 1, \ldots, N_L \tag{9}$$

where V_i denotes the voltage magnitude at the i^{th} bus, $V_{max,i}$ and $V_{min,i}$ represent the voltage limits of the i^{th} bus, respectively; and $I_{max,k}$ denotes the current limit of the k^{th} branch.

3) *DG capacity limits:* The DG capacities must be in the permissible ranges:

$$P_{DG\min,i} \le P_{DG,i} \le P_{DG\max,i}, \quad i = 1, \ldots, N_{DG} \tag{10}$$

where $P_{DG\min,i}$ and $P_{DG\max,i}$ denote the power limits of the i^{th} DG, respectively.

4) *DG penetration limits:* The minimum and maximum DG penetration levels to an RDN are defined as 10% and 60% of the total active power load demand of that network, respectively [25]. The threshold 10% chosen is to maintain the existence of DGs in the network for their impact evaluation while the selection of threshold 60% is to prevent the network from reverse power flow situation due to excessive penetration of DGs. These can be demonstrated by the following equation:

$$0.1 \times \sum_{j=2}^{N_B} P_{D,j} \le \sum_{i=1}^{N_{DG}} P_{DG,i} \le 0.6 \times \sum_{j=2}^{N_B} P_{D,j} \tag{11}$$

5) *Radial configuration constraint:* After reconfiguration, the distribution network must ensure radial configuration and all loads are served [5], [41]:

$$\det(A) = \begin{cases} 1 \text{ or } -1 & \text{(radial system)} \\ 0 & \text{(not radial)} \end{cases} \tag{12}$$

where A denotes a matrix indicating the connection of branches and buses in the network. A_{ij} is set to -1 or 1 if the i^{th} branch is connected from/to the j^{th} bus; otherwise, A_{ij} is set to 0.

III. QUASI-OPPOSITIONAL CHAOTIC NEURAL NETWORK ALGORITHM

A. NNA

1) INITIAL POPULATION

In the search space, the initial population of pattern solutions X are randomly created as the following matrix:

$$X = \begin{bmatrix} x_1^1 & x_2^1 & \cdots & x_N^1 \\ x_1^2 & x_2^2 & \cdots & x_N^2 \\ \vdots & \vdots & \vdots & \vdots \\ x_1^{N_P} & x_2^{N_P} & \cdots & x_N^{N_P} \end{bmatrix} \tag{13}$$

where N_P is the population size and N is the number of decision variables. After initial population initialization, fitness function values of pattern solutions are defined. Then, the best pattern solution having the best fitness function value is determined as the target solution (X_{Target}).

2) WEIGHT MATRIX

In order to generate new candidate solutions, each pattern solution is assigned a corresponding weight vector, and initial weights are determined as follows:

$$W^t = [W_1, W_2, \ldots, W_{N_P}] = \begin{bmatrix} w_1^1 & w_2^1 & \cdots & w_N^1 \\ w_1^2 & w_2^2 & \cdots & w_N^2 \\ \vdots & \vdots & \vdots & \vdots \\ w_1^{N_P} & w_2^{N_P} & \cdots & w_N^{N_P} \end{bmatrix} \tag{14}$$

where W^t is a square matrix at the t^{th} iteration that generates uniform random numbers from 0 to 1 over iterations.

To control the creation of new pattern solutions and bias of movement, the sum of the weights for a pattern solution is

TABLE 1. The pseudocode of bias strategy in NNA.

Algorithm 1: Pseudocode of bias operator strategy

```
% N_b is the number of biased variables in population of new pattern solution
% N_wb is the number of biased variables in updated weight matrix
% [LB, UB] is the search boundary
for i = 1 : N_P
    if rand ≤ β
        % Bias for new pattern solutions %
        N_b = round(N × β)
        for j = 1 : N_b
            X_Input(i, Integer rand[0, N]) = LB + (UB − LB) × rand
        end for
        % Bias for updated weight matrix %
        N_wb = round(N_P × β)
        for j = 1 : N_wb
            W_Updated(j, Integer rand[0, N_P]) = U(0,1)
        end for
    end if
end for
```

TABLE 2. The pseudocode of NNA.

Algorithm 2: Pseudocode of NNA

```
Initialize the initial parameters of the NNA (N_P and T_max)
Randomly generate an initial population of pattern solutions
Calculate the fitness function values of initial pattern solutions
Randomly generate the weight matrix considering the imposed constraints in Eqs. (15) and (16)
Define target solution (X_Target) and its corresponding target weight (W_Target)
for t = 1 : T_max
    Generate new pattern solutions (X_New) using Eqs. (17) and (18)
    Update the weight matrix (W) using Eq. (19)
    for i = 1 : N_P
        if rand ≤ β
            Perform the bias operator using Algorithm 1
        else (rand > β)
            Apply the transfer function operator using Eq. (21)
        end if
    end for
    Calculate the fitness function values for all updated pattern solutions
    Update the target solution and its corresponding target weight
    Update the value of β using Eq. (20)
end for
Return the target solution X_Target and its corresponding fitness function value
```

subject to the following constraint:

$$\sum_{j=1}^{N_P} w_{ij}^t = 1, \quad i = 1, 2, \ldots, N_P \tag{15}$$

where

$$w_{ij} \in U[0, 1], \quad i, j = 1, 2, \ldots, N_P \tag{16}$$

This constraint is imposed to allow pattern solutions of NNA to control movement with slight bias (changing from 0 to 1). After creating initial weights, the weight corresponding to the target solution (X_{Target}), called the target weight (W_{Target}), is selected from the weight matrix W in Eq. (14).

New pattern solutions at the $(t+1)^{\text{th}}$ iteration are generated and updated as follows:

$$X_{j,New}^{t+1} = \sum_{j=1}^{N_P} w_{ij}^t \times X_i^t, \quad j = 1, 2, \ldots, N_P \tag{17}$$

$$X_i^{t+1} = X_i^t + X_{i,New}^{t+1}; \quad i = 1, 2, \ldots, N_P \tag{18}$$

The weight matrix is then updated based on the target weight (W_{Target}) as the following equation:

$$W_i^{t+1} = W_i^t + 2 \times rand(0, 1) \times [W_{Target}^t - W_i^t], \quad i = 1, 2, \ldots, N_P \tag{19}$$

During the optimization process, the weight matrix must satisfy the imposed constraints in Eqs. (15) and (16).

3) BIAS OPERATOR

To explore the design domain, a bias operator is applied to adjust the probability of pattern solutions created in the new population and updated weight matrix. By virtue of its role, the algorithm is prevented from premature convergence (particularly in initial iterations). Table 1 gives the Pseudocode of bias strategy in NNA.

Modification factor β defines the probability of the pattern solutions to be adjusted. The value of β is initially set to 1, and the value of β is reduced at each iteration as follows [36]:

$$\beta^{t+1} = \beta^t \times 0.99, \quad t = 1, 2, \ldots, T_{\max} \tag{20}$$

When reducing operator bias adaptively, the algorithm tends to search for optimal solutions close to the target solution (X_{Target}) and avoids drastic changes in the pattern solutions in the last iterations.

4) TRANSFER FUNCTION OPERATOR

To create better quality solutions toward the target solution, the transfer function operator transfers the new pattern solutions from their current positions to new positions closer to the target solution (X_{Target}) in the search space. Hence, the proposed method for a transfer function operator (TF) is defined as follows:

$$X_{i,\text{Updated}}^{t+1} = X_i^{t+1} + 2 \times rand(0, 1) \times [X_{Target}^t - X_i^{t+1}], \quad i = 1, 2, \ldots, N_P \tag{21}$$

The bias operator has more opportunities to create new pattern solutions to explore unvisited pattern solutions in the first iterations. However, the chance for the bias operator is decreasing as the number of iterations goes up, and the transfer function operator has more opportunities to exploit towards target solutions. Table 2 presents the Pseudocode of NNA.

B. THE QOBL STRATEGY

The theory of opposition-based learning (OBL) was first introduced by Tizhoosh [42]. The OBL strategy considers concurrently existing guesses and its opposite guesses to better approximate existing candidate solutions. Moreover, the

TABLE 3. The pseudocode of QOBL approach.

Algorithm 3: Pseudocode of QOBL strategy

```
% OX_ij is opposite point of X_ij
% QOX_ij is the quasi-opposite point of X_ij
% [LB, UB] is the search boundary
for i = 1 : N_P
    for j = 1 : N
        OX_ij = LB_j + UB_j – X_ij
        M_ij = LB_j + (UB_j – LB_j) / 2
        if (X_ij < M_ij)
            QOX_ij = M_ij + (OX_ij – M_ij) × rand
        else
            QOX_ij = OX_ij + (M_ij – OX_ij) × rand
        end if
    end for
end for
```

TABLE 4. The pseudocode of CLS approach.

Algorithm 4: Pseudocode of CLS strategy

```
Set CLS limit K
Initialize the chaotic sequence by generating Z_o using Eq. (20)
for k = 1 : K
    Update the chaotic sequence Z_k using Eq. (21)
    Randomly select two pattern solutions X_i and X_j from current population
    Generate a new target solution (X_NewTarget) using Eq. (22)
    Calculate fitness function value for new solution
    if fitness(X_NewTarget) < fitness(X_Target)
        X_Target = X_NewTarget
        fitness(X_Target) = fitness(X_NewTarget)
    end if
end for
```

theory of OBL was further developed into QOBL, showing that QOBL can be more effective than OBL for obtaining global optimal solutions [43]. The QOBL is integrated into metaheuristic methods to improve solution quality and convergence speed.

Based on a population of pattern solutions X_{ij}, the opposite point OX_{ij} of X_{ij} is then generated as follows [42]:

$$QX_{ij} = LB_j + UB_j - X_{ij} \tag{22}$$

Finally, the quasi-opposite point QOX_{ij} of OX_{ij} can be defined as follows [43]:

$$QOX_{ij} = rand\left(\frac{LB_i + UB_i}{2}, OX_{ij}\right) \tag{23}$$

In this study, QOBL is used in two phases of QOCNNA: population initialization and generation jumping. As for QOBL population initialization, the algorithm creates a quasi-oppositional population of the randomly generated initial population. Then, randomly created initial population and their quasi-oppositional population are considered simultaneously to define the best solutions for the initial population. As for QOBL generation jumping, the search process of the algorithm may be driven to jump to quasi-oppositional solutions that have better fitness function values. In this step, jumping rate j_r is used to decide whether to jump to the quasi-oppositional solutions or keep current solutions. Table 3 depicts the Pseudocode of the QOBL approach.

C. THE CLS STRATEGY

Chaos is randomness created by simple deterministic systems. In QOCNNA, the chaotic sequence is employed to boost searchability and to prevent the algorithm from getting stuck into the local optimization. An initial chaotic value is defined as follows:

$$Z_0 = rand(0, 1) \tag{24}$$

The following values of that chaotic sequence using a logistic map are given as the following equation [44]:

$$Z_{k+1} = \mu \times Z_k \times (1 - Z_k) \tag{25}$$

where $Z_k \in (0, 1) \forall k \in \{0, 1, 2, \ldots\}$ and $\mu \in (0, 4]$.

The CLS strategy is integrated to accelerate the search process by exploring the neighborhood of the current target solution (i.e., best solution). Hence, a new candidate solution is created as follows [45]:

$$X_{\text{NewTarget},k} = X_{\text{Target},k} + (Z_k - 0.5) \times (X_{i,k} - X_{j,k}) \tag{26}$$

where $X_{\text{Target},k}$ and $X_{\text{NewTarget},k}$ are the current target solution and the new target solution created at the k^{th} CLS iteration, respectively; $X_{i,k}$ and $X_{j,k}$ are the two solutions randomly selected from the current population, respectively; and Z_k is the chaotic variable at the k^{th} iteration. If fitness function value of $X_{\text{NewTarget},k}$ is better than that of $X_{\text{Target},k}$, $X_{\text{NewTarget},k}$ will replace $X_{\text{Target},k}$ in the population. The CLS strategy is executed until the CLS limit (K) is satisfied. The Pseudocode of the CLS strategy is given in Table 4.

D. THE PROPOSED QOCNNA

In this study, the original NNA is combined with QOBL and CLS strategies to develop an improved version of NNA called QOCNNA. Initially, QOCNNA randomly generates a population of pattern solutions $\boldsymbol{X}$. The QOBL is then employed to create the quasi-opposite population $\boldsymbol{QOX}$ of the initial population. Afterwards, QOCNNA combines two sets of $\boldsymbol{X}$ and $\boldsymbol{QOX}$, and then the N_P best solutions from the combined set $\{\boldsymbol{X}, \boldsymbol{QOX}\}$ are selected for the initial population. Next, the same search process as NNA is implemented to create a new population of pattern solutions and to update the weight matrix. Based on jumping rate j_r, QOBL may be used to help QOCNNA transition to better quasi-oppositional solutions of current pattern solutions. Lastly, the CLS is implemented to obtain a better target solution. The optimization process is executed until satisfying stopping criteria. QOCNNA pseudocode is presented in Table 5.

IV. APPLICATION OF QOCNNA TO SNR-DG PROBLEM

A. INITIALIZATION

Each pattern solution of the initial population in QOCNNA represents a solution vector for the SNR-DG problem consisting of opened switches, locations of sizes of DGs. Hence,

TABLE 5. The pseudocode of QOCNNA.

Algorithm 5: Pseudocode of QOCNNA

Initialize the initial parameters of the QOCNNA (N_P, $T_{\max}$, j_r, and K)
% QOBL based population initialization %
Randomly generate an initial population X
Generate quasi-opposite solutions QOX_i of initial pattern solutions X_i using Algorithm 3
Calculate the fitness function values of combined set $\{\boldsymbol{X}, \boldsymbol{QOX}\}$ and sort them
Select the N_P best solutions from the set $\{\boldsymbol{X}, \boldsymbol{QOX}\}$ as initial population
Randomly generate the weight matrix considering the imposed constraints in Eqs. (15) and (16)
Define target solution (X_{Target}) and its corresponding target weight (W_{Target})
for $t = 1 : T_{\max}$
  % Search process of NNA %
  Generate new pattern solutions (X_{New}) using Eqs. (17) and (18)
  Update the weight matrix (W) using Eq. (19)
  for $i = 1 : N_P$
    if $rand \leq \beta$
      Perform the bias operator using Algorithm 1
    else ($rand > \beta$)
      Apply the transfer function operator using Eq. (21)
    end if
  end for
  Calculate the fitness function values for all updated pattern solutions
  Update the value of β using Eq. (20)
  % QOBL based generation jumping %
  if $rand < j_r$
  Generate quasi-opposite solutions QOX_i of updated pattern solutions X_i using Algorithm 3
  Calculate the fitness function values for quasi-opposite solutions QOX_i
    if $fit(QOX_i) < fit(X_i)$
      $X_i = QOX_i$
      $fit(X_i) = fit(QOX_i)$
    end if
  end if
  % Chaotic local search %
  Update the target solution and its corresponding target weight
  Perform the CLS strategy to generate better target solution using Algorithm 4
end for
Return the target solution X_{Target} and its corresponding fitness function value

the i^{th} solution vector is expressed as follows:

$$X_i = [S_1, \ldots, S_{N_{SW}}, L_1, \ldots, L_{N_{DG}}, P_1, \ldots, P_{N_{DG}}], \quad i = 1, \ldots, N_P \tag{27}$$

where S, L, and P are opened switches, the locations and sizes of DGs, respectively, N_{SW} denotes the number of opened switches.

To start QOCNNA, the initial population are randomly initialized within the design space as follows:

$$S_i = round[S_{i,\min} + rand(0, 1) \times (S_{i,\max} - S_{i,\min})], \quad i = 1, \ldots, N_{SW} \tag{28}$$

$$L_j = round[L_{j,\min} + rand(0, 1) \times (L_{j,\max} - L_{j,\min})], \quad j = 1, \ldots, N_{DG} \tag{29}$$

$$P_j = P_{j,\min} + rand(0, 1) \times (P_{j,\max} - P_{j,\min}), \quad j = 1, \ldots, N_{DG} \tag{30}$$

where $S_{i,\min}$ is equal to 1 and $S_{i,\max}$ is the length of the i^{th} fundamental loop vectors. The principle of the fundamental loop vectors can be found in [30]. $L_{j,\min}$ is equal to 2, indicating that DGs may be integrated to all buses except the slack bus. According to Eqs. (28) and (29), values for opened switches (S_i) and locations of DGs (L_j) are rounded due to their integer nature.

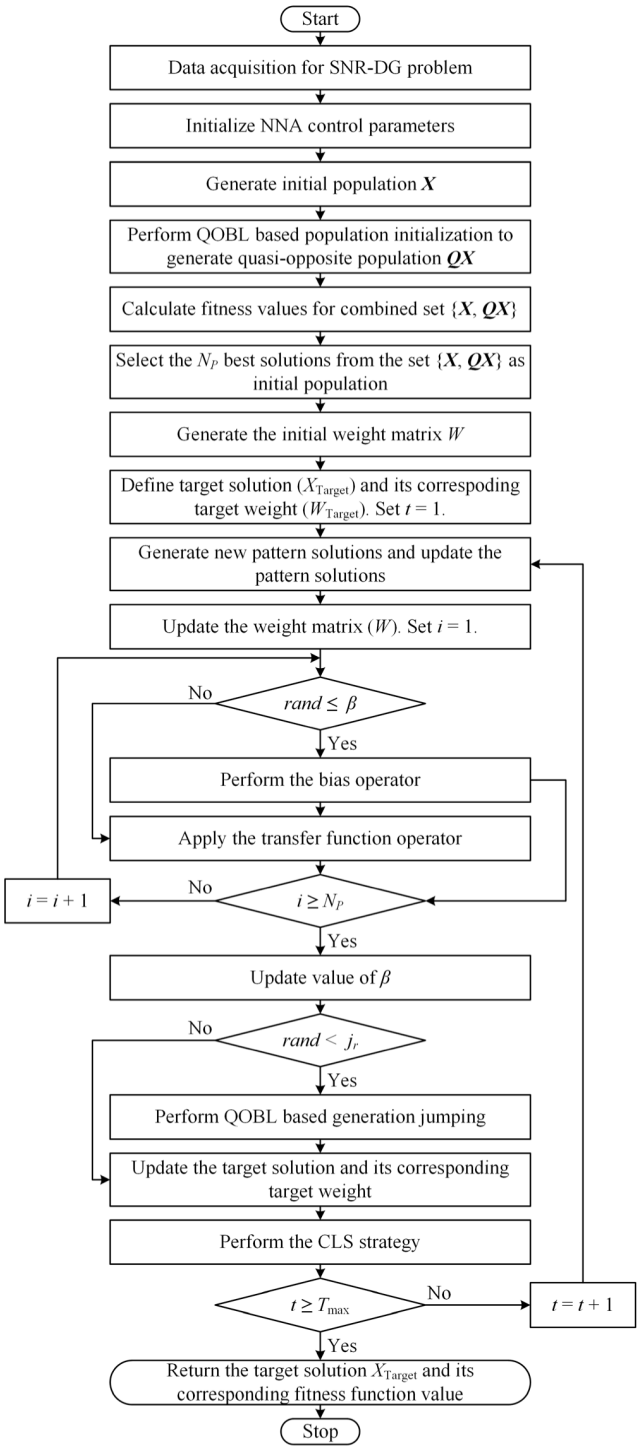

FIGURE 2. Flowchart of QOCNNA for solving the SNR-DG problem.

B. FITNESS FUNCTION VALUE

The fitness function value (FF) of each pattern solution can be obtained as follows:

$$FF = OF + K \sum_{i=1}^{N_B} (V_i - V_i^{\lim})^2$$

$$FF = +K\sum_{k=1}^{N_L}(I_k - I_k^{\lim})^2 + K(PE_{DG} - PE_{DG}^{\lim})^2 \quad (31)$$

where K embodies penalty constants for inequality constraint violations and is set to 10^3 in this study. The limit values of bus voltages (V_i), currents (I_k), and DG penetration (PE) are expressed as the following equation:

$$x^{\lim} = \begin{cases} x_{\max} & \text{if } x > x_{\max} \\ x_{\min} & \text{if } x < x_{\min} \\ x & \text{otherwise} \end{cases} \quad (32)$$

where x signifies the values of V_i, I_k, and PE_{DG}, and $x^{\lim}$ signifies their limitations, respectively.

C. OVERALL PROCEDURE

QOCNNA implementation steps for the SNR-DG problem can be summarized as follows:

Step 1: Data acquisition for SNR-DG problem includes detailed data of test systems (load data and branch data), allowable limits for control variables (opened switches, locations and sizes of DGs), and operational constraints;

Step 2: Select the control parameters of QOCNNA (N_P, $T_{\max}$, j_r, and K);

Step 3: Generate randomly initial population $\boldsymbol{X}$ of N_P pattern solutions as in Section 4.1. Implement the QOBL approach to create a quasi-opposite population $\boldsymbol{QOX}$. Calculate fitness function values using Eq. (31) for all solutions in $\boldsymbol{X}$ and $\boldsymbol{QOX}$. Select the N_P best solutions from the set $\{\boldsymbol{X}, \boldsymbol{QOX}\}$ for the initial population;

Step 4: Create the initial weight matrix randomly as Eq. (14), satisfying the imposed constraint according to Eqs. (15) and (16);

Step 5: Define target solution (X_{Target}) having the best fitness function value and its corresponding target weight (W_{Target}). Set $t = 0$;

Step 6: Start the main loop, $t = t + 1$;

Step 7: Create new pattern solutions and update the pattern solutions as Eqs. (17) and (18);

Step 8: Update the weight matrix (W) via Eq. (19);

Step 9: If $rand \leq \beta$, perform the bias operator to update new pattern solutions and weight matrix using Algorithm 1. Otherwise, perform the transfer function operator to update the new position of pattern solutions according to Eq. (21);

Step 10: Update modification factor β using Eq. (20);

Step 11: Check the jumping rate condition. If $rand < j_r$, implement the QOBL approach to obtain quasi-opposite points of the current population. Evaluate fitness function values of quasi-oppositional solutions and select better solutions for new population;

Step 12: Update target weight corresponding to the target solution;

Step 13: Perform the CLS strategy to create a better target solution;

Step 14: If $t \geq T_{\max}$, stop the optimization process; otherwise, back to Step 6.

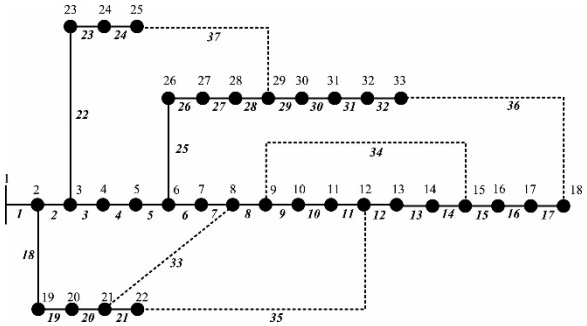

FIGURE 3. The IEEE 33-bus RDN.

Fig. 2 depicts the flowchart of QOCNNA for solving the SNR-DG problem.

V. SIMULATION RESULTS

This study validates the performance of the proposed QOCNNA on 33-bus, 69-bus, and 118-bus RDNs. In scenario 1, active power loss minimization is considered as a single objective function, where the weighting factors w_1 and w_2 in Eq. (5) are set to 1 and 0, respectively. For scenario 1, three cases at three load conditions are considered for an in-depth study. Cases 1 and 2 study NR and DGs installation problems separately, while case 3 investigates these two problems concurrently as a combined optimization problem. In scenario 2, active power loss minimization and voltage stability index maximization is considered as a multi-objective function, where w_1 and w_2 are set to 0.7 and 0.3, respectively, as proposed in Ref [25]. Moreover, the considered load conditions are as follows: light load (0.5), nominal load (1.0), and heavy load (1.6). In addition, a practical scenario relative to daily variable load demand and generation has also been considered with the objective of total annual energy loss minimization. The voltage magnitudes at load buses must not exceed $\pm 10\%$ of the rated voltage for case studies. For 33-bus and 69-bus RDNs, the number of DGs is fixed to 3 with the size of each one ranging from 0 to 3 MW. Meanwhile, the number of DGs is 5 where the maximum size of each DG is 5 MW for 118-bus RDN.

QOCNNA is implemented on MATLAB 2019a, and Matpower 6.0 toolbox [46] is deployed to compute the load flow. The control parameters of QOCNNA contain a population size (N_P), a maximum number of iterations ($T_{\max}$), jumping rate (j_r), and maximum iterations of chaotic local search (K), which are respectively set as follows: $N_P = 50$ (for 33- and 69-bus RDNs) and $N_P = 100$ (for 118-bus RDN), $T_{\max} = 200$, $j_r = 0.3$, and $K = 20$. Moreover, QOCNNA is performed 30 times independently for each case study. To confirm the results of QOCNNA, the original NNA, ant lion optimizer (ALO) [37], whale optimization algorithm (WOA) [38], and sine cosine algorithm (SCA) [39] are also implemented for the SNR-DG problem. These methods also use the same population size and maximum number of iterations as QOCNNA for the same experimental system.

TABLE 6. Simulation results of QOCNNA for scenario 1 of 33-bus RDN.

Case study	Items	Load level		
		Light (0.5)	Nominal (1.0)	Heavy (1.6)
Initial case	Opened switches	33-34-35-36-37	33-34-35-36-37	33-34-35-36-37
	P_L (kW)	47.07	202.68	575.36
	V_{min} (p.u)	0.9583	0.9131	0.8528
Case 1	Opened switches	7-9-14-32-37	7-9-14-32-37	7-9-14-28-32
	P_L (kW)	33.2690	139.5513	381.2398
	PLR (%)	29.3213	31.1460	33.7391
	V_{min} (p.u)	0.9698	0.9378	0.9027
Case 2	Opened switches	33-34-35-36-37	33-34-35-36-37	33-34-35-36-37
	P_{DG}/(Bus) (MW)	0.3509/ (14) 0.2875/ (25) 0.4761/ (30)	0.7050/ (14) 0.5702/ (25) 0.9538/ (30)	1.1180/ (14) 0.8873/ (25) 1.5611/ (30)
	P_L (kW)	18.1929	75.4237	202.1933
	PLR (%)	61.3499	62.7863	64.8581
	V_{min} (p.u)	0.9815	0.9622	0.9384
Case 3	Opened switches	11-28-31-33-34	7-9-14-27-30	7-9-14-28-31
	P_{DG}/(Bus) (MW)	0.2547/ (8) 0.2982/ (18) 0.5616/ (25)	0.4822/ (12) 1.0153/ (25) 0.7315/ (33)	0.7318/ (12) 1.8961/ (25) 0.9386/ (33)
	P_L (kW)	13.5084	54.6942	144.9139
	PLR (%)	71.3018	73.0141	74.8134
	V_{min} (p.u)	0.9835	0.9674	0.9559

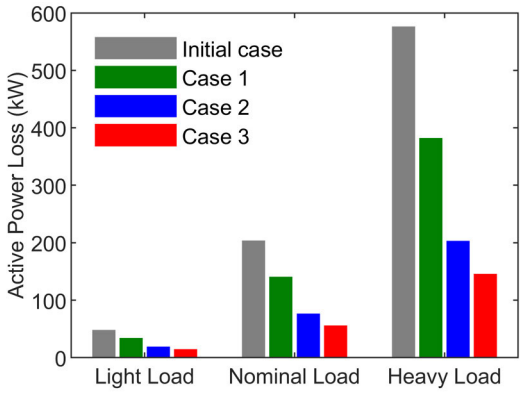

FIGURE 4. Active power loss for scenario 1 of 33-bus RDN at three load conditions.

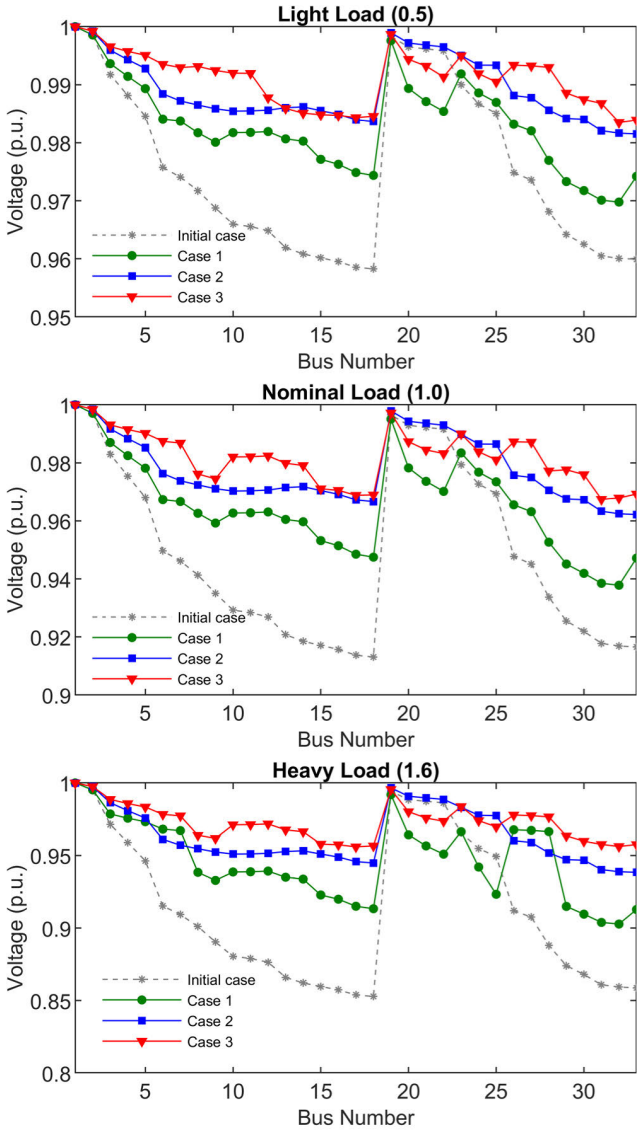

FIGURE 5. Voltage profiles for scenario 1 of 33-bus RDN at three load conditions.

A. 33-BUS RDN

The 33-bus RDN is a small-scale system with a voltage level of 12.66 kV, 37 branches, 32 closed switches, and 5 opened switches [47]. The single line diagram of the 33-bus RDN is shown in Fig. 3. For base configuration, the total active and reactive loads of 33-bus RDN are 3.73 MW and 2.3 MVAr, respectively.

1) SCENARIO 1: ACTIVE POWER LOSS MINIMIZATION

In this scenario, QOCNNA is applied to minimize active power loss as a single objective function. Three different cases with three load conditions of light (0.5), nominal (1.0), and heavy (1.6) are considered. Table 6 details the numerical results found by QOCNNA for 33-bus RDN. Figs. 4 and 5 depict active power losses and voltage profiles for all cases of scenario 1 of 33-bus RDN at three load conditions, respectively. In the case of light load condition, the active power loss from the initial case is 47.07 kW, which is reduced to 33.2690 kW, 18.1929 kW, and 13.5084 kW for cases 1, 2, and 3, respectively. As a result, the power loss reduction (PLR) percentages associated with cases 1, 2, and 3 are 29.3213%, 61.3499%, and 71.3018%. Similarly, at nominal load condition, the active power loss of the initial case is reduced from 202.68 kW to 139.5513 kW, 75.4237 kW, and 54.6942 kW, which leads to PLR of 31.1460%, 62.7863%, and 73.0141% corresponding to cases 1, 2, and 3, respectively. Notably, in comparison with the initial case, PLR for cases 1, 2, and 3 at heavy load condition are 33.7391%, 64.8581%, and 74.8134%, respectively. Moreover, significant improvements in the voltage profile of the system for

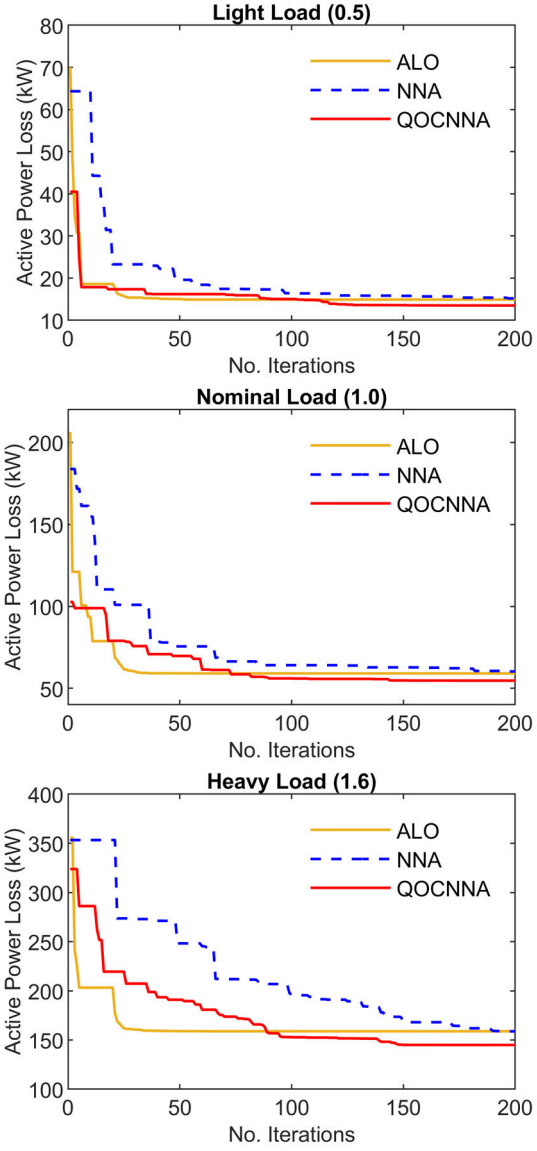

FIGURE 6. Convergence characteristics of QOCNNA, NNA and ALO for case 3 of scenario 1 of 33-bus RDN.

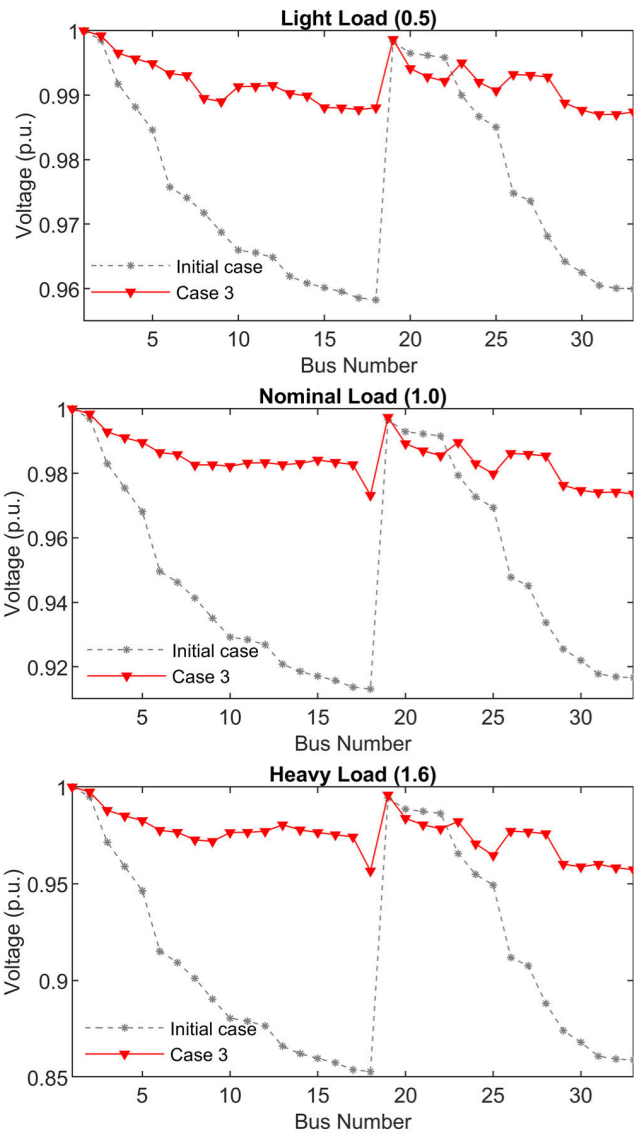

FIGURE 7. Voltage profiles for scenario 2 of 33-bus RDN at three load conditions.

three cases at all load conditions are also obtained, as shown in Fig. 5.

In case 1, changing positions of opened and closed switches contribute to modifying the power flow paths, which is the main reason for such power loss reductions. As a result, the distribution of power is realized through low resistance roots; therefore, power loss and voltage profile are improved. Meanwhile, in case 2, DG units provide local power supply, resulting in reduced power flows through the branches, which is the main reason for the improved system performance. From Table 1, improvement in PLR and voltage profile for case 2 are higher when compared to case 1. It shows that the DG installation offers more desirable results of maximum PLR compared to the NR implementation. Finally, a combination of NR and DG installation is studied in case 3. As shown in Table 1, Figs. 4 and 5, the optimal results in case 3 are better than cases 1 and 2 at all load conditions in terms of reduced power loss and improved voltage profile. Therefore, it shows that combining NR with the DGs installation in the SNR-DG problem would yield better results than considering each problem individually.

Table 7 presents comparisons between the proposed QOCNNA and other methods at all load conditions for case 3 of 33-bus RDN. At light load condition, QOCNNA yields opened switches {11-28-31-33-34}, DG locations at 8^{th}, 18^{th}, and 25^{th} buses with the DG sizes of 0.2547 MW, 0.2982 MW, and 0.5616 MW. As a result, QOCNNA acquires an active power loss of 13.5084 kW, which is much lower than 15.1660 kW from NNA, 14.9030 kW from ALO, 15.17 kW from EOA [17], 14.51 kW from IEOA [17], 16.24 kW from ISCA [25], 17.78 kW from HSA [26],

TABLE 7. Comparative results of QOCNNA and other methods for case 3 of scenario 1 of 33-bus RDN.

Load level	Methods	Opened switches	Sum P_{DG} (MW)	P_L (kW)	PLR (%)	Standard deviation
Light (0.5)	Initial case	33-34-35-36-37	-	47.07	-	-
	QOCNNA	11-28-31-33-34	1.1145	13.5084	71.3018	0.6772
	NNA	8-17-28-33-34	1.0595	15.1660	67.7804	0.7200
	ALO	7-9-28-32-35	1.1145	14.9030	68.3392	0.9015
	EOA [17]	6-28-34-35-36	1.114	15.17	67.76	-
	IEOA [17]	8-28-32-33-34	1.106	14.51	69.17	-
	ISCA [25]	7-10-14-28-31	0.7867	16.24	65.49	-
	HSA [26]	7-10-14-28-32	0.8898	17.78	62.22	-
	FWA [28]	7-10-14-28-32	0.8607	16.22	65.53	-
Nominal (1.0)	Initial case	33-34-35-36-37	-	202.68	-	-
	QOCNNA	7-9-14-27-30	2.2290	54.6942	73.0141	2.5251
	NNA	10-14-28-32-33	2.2274	60.2994	70.2485	3.9668
	ALO	7-11-26-30-34	2.2290	59.0788	70.8508	6.9868
	EOA [17]	8-27-33-34-36	2.229	61.48	69.66	-
	IEOA [17]	7-10-13-27-31	2.228	57.40	71.67	-
	ISCA [25]	7-9-14-28-31	1.6912	66.81	67.03	-
	HSA [26]	4-7-10-28-32	1.6684	73.05	63.95	-
	GA [26]	7-10-28-32-34	1.9633	75.13	62.92	-
	RGA [26]	7-9-12-27-32	1.774	74.32	63.33	-
	FWA [28]	7-11-14-28-32	1.6841	67.11	66.89	-
	FF [33]	8-9-28-32-33	1.7738	73.95	63.51	-
Heavy (1.6)	Initial case	33-34-35-36-37	-	575.36	-	-
	QOCNNA	7-9-14-28-31	3.5664	144.9139	74.8134	7.0850
	NNA	7-8-9-17-28	3.5586	158.8140	72.3975	8.1438
	ALO	7-12-27-32-35	3.5664	158.8809	72.3859	10.7827
	EOA [17]	10-28-30-33-34	3552	152.26	73.54	-
	IEOA [17]	7-9-14-27-31	3566	148.42	74.19	-
	ISCA [25]	7-9-14-28-31	2.9812	167.96	70.81	-
	HSA [26]	7-10-14-28-32	2.7529	194.22	66.23	-
	FWA [28]	7-10-14-28-32	2.7529	172.97	69.93	-

and 16.22 kW from FWA [28] for this load condition. At normal load condition, QOCNNA optimizes the NR with opened switches {7-9-14-27-30}. Moreover, DGs are connected to 12th, 25th, and 33rd buses corresponding to 0.4822 MW, 1.0153 MW, and 0.7315 MW DG sizes. QOCNNA obtains the best active power loss for this load condition among compared algorithms, as shown in Table 7. At heavy load condition, opened switches {7-9-14-28-31} is obtained by QOCNNA to create the optimal NR. DGs are linked to 12th, 25th, and 33rd buses with 0.7318 MW, 1.8961 MW, and 0.9386 MW DG sizes. For the heavy load condition, QOCNNA obtains the lowest active power loss (144.9139 kW) in comparison with NNA (158.8140 kW), ALO (158.8809 kW), EOA [17] (152.26 kW), IEOA [17] (148.42 kW), ISCA [25] (167.96 kW) HSA [26] (194.22 kW), and FWA [28] (172.97 kW). As shown in the 7th column of Table 7, QOCNNA possesses smaller standard deviations of solutions than NNA and ALO for all loading conditions, which proves that QOCNNA is more robust than NNA and ALO for these case studies.

From the comparisons in Table 7, the proposed QOCNNA offers the highest solution accuracy among the compared methods due to the attainment of minimum objective value for the 33-bus system at all load conditions. It is worth highlighting that the superiority of QOCNNA over NNA in terms of solution quality, proving the integrated improvement strategies contribute to enhance the search ability of NNA. Moreover, Fig. 6 presents the convergence curves provided by QOCNNA, NNA, and ALO for case 3 at all load conditions, which show that QOCNNA has better convergence characteristics than NNA and ALO. In initial iterations, NNA illustrates a slow convergence speed because bias values used in these iterations are sufficiently large to mainly perform exploration via the bias operator. In later iterations, NNA primarily implements exploitation as bias factor is reduced to lower values. Meanwhile, QOCNNA manifests a significant improvement in convergence speed in the initial iterations thanks to integrated CLS strategy, which enhances the exploitation of QOCNNA. Further, QOCNNA finds the final solution with higher accuracy. This proves that adopting the QOBL strategy helps QOCNNA achieve a good balance between exploration and exploitation in the later iterations. Compared to ALO, QOCNNA performs the search more effectively for all cases of this scenario based on lower objective values obtained. Therefore, QOCNNA improves its performance compared to the original NNA and ALO for solution quality and convergence characteristics.

2) SCENARIO 2: ACTIVE POWER LOSS AND OVSI OPTIMIZATION

In scenario 2, QOCNNA is implemented to the SNR-DG problem (i.e., case 3) for the multi-objective scenario of active power loss and OVSI, where loading levels of 0.5 (light), 1.0 (nominal), 1.6 (heavy) are investigated. Table 8 displays the optimal results obtained by QOCNNA. PLR for case 3 at

TABLE 8. Comparative results of QOCNNA and other methods for scenario 2 of 33-bus RDN.

Load level	Methods	Opened switches	P_{DG}/(Bus)	P_L (kW)	PLR (%)	OVSI	OVSI (%)	Fitness function	Standard deviation	V_{min} (p.u)
Light (0.5)	Initial case	33-34-35-36-37	-	47.07	-	28.8819	-	-	-	0.9583
	QOCNNA	7-9-14-28-31	0.2223/ (12) 0.3123/ (18) 0.5799/ (25)	13.3706	71.5947	30.9625	7.2037	0.4787	0.0087	0.9870
	NNA	7-14-28-32-35	0.4514/ (9) 0.6341/ (29) 0.0290/ (33)	15.0311	68.0670	30.8950	6.9697	0.5040	0.0160	0.9853
	ALO	9-28-32-33-34	0.5938/ (25) 0.2214/ (26) 0.2993/ (13)	14.5961	68.9911	30.8763	6.9053	0.4977	0.0265	0.9828
	ISCA [25]	7-9-14-28-32	0.3397/ (30) 0.2054/ (18) 0.3241/ (20)	17.68	62.44	30.93	6.49	0.5431	-	-
Nominal (1.0)	Initial case	33-34-35-36-37	-	202.68	-	25.8581	-	-	-	0.9131
	QOCNNA	7-10-12-17-28	0.6521/ (32) 0.9343/ (25) 0.6426/ (15)	59.1855	70.7981	30.0893	16.3629	0.4622	0.0051	0.9732
	NNA	6-10-14-17-28	0.1451/ (14) 1.2816/ (30) 0.8023/ (8)	61.8983	69.4597	29.9359	15.7696	0.4729	0.0059	0.9672
	ALO	7-11-14-28-32	0.5768/ (9) 1.1913 / (30) 0.4608/ (22)	60.8613	69.9713	29.9176	15.6991	0.4695	0.0225	0.9715
	ISCA [25]	7-9-14-28-31	0.6217/ (30) 0.7266/ (18) 0.4362/ (20)	67.57	66.66	29.97	14.51	0.4922	-	0.9678
Heavy (1.6)	Initial case	33-34-35-36-37	-	575.36	-	22.3449	-	-	-	0.8528
	QOCNNA	7-9-17-28-34	1.1517/ (13) 0.9858/ (25) 1.4286/ (31)	161.3266	71.9608	29.0555	30.0315	0.4270	0.0068	0.9565
	NNA	11-14-17-27-33	1.0946/ (9) 0.5042/ (33) 1.9677/ (29)	166.3376	71.0899	28.8648	29.1783	0.4346	0.0105	0.9520
	ALO	7-9-14-17-27	2.2617/ (30) 0.6558 / (12) 0.6489/ (9)	166.1195	71.1278	28.8826	29.2579	0.4342	0.0149	0.9476
	ISCA [25]	7-9-14-28-31	0.1097/ (30) 0.1154/ (18) 0.1018/ (20)	171.58	70.18	29	27.08	0.4399	-	0.9502

light, nominal and heavy loadings are 71.5947%, 70.7981%, and 71.9608%, respectively. Meanwhile, the improvement in OVSI for increasing load levels are 7.2037%, 16.3629%, and 30.0315%, respectively. It can be seen that active power loss and OVSI are better enhanced than the initial case. Hence, QOCNNA is capable of providing a good compromised solution for consideration of both active power loss and OVSI objectives. Fig. 7 presents the voltage profile of the system for light, nominal and heavy loadings for the initial case and after the SNR-DG, which shows bus voltages are completely improved. Accordingly, the minimum voltages are improved to 0.9870 p.u., 0.9732 p.u., 0.9565 p.u. for light, nominal and heavy loadings, respectively.

The results yielded from the QOCNNA are compared to those from NNA, ALO, and ISCA [25] as in Table 8. QOCNNA yields a lower active power loss than that from NNA, ALO, and ISCA [25] for light load condition while the OVSI value obtained by the QOCNNA is slightly better than those from NNA and ALO, and much better than that from ISCA [25]. From the optimal results, QOCNNA has a better solution than NNA, ALO, and ISCA [25] for both active power loss and OVSI objectives for light load condition. For the nominal load condition, active power loss obtained by QOCNNA, NNA, ALO, and ISCA [25] respectively are 59.1855 kW, 61.8983 kW, 60.8613 kW, and 67.57 kW, which leads to PLRs being 70.7981%, 69.4597%, 69.9713%, and 66.66%, respectively. Obviously, PLR obtained by QOCNNA is better than those obtained by other techniques. Likewise, the OVSI values (in p.u.) found by the QOCNNA, NNA, ALO, and ISCA [25] are 30.0893, 29.9359, 29.9176, and 29.97, respectively. Hence, QOCNNA can provide a better result for active power loss and OVSI objectives than NNA, ALO, and ISCA [25]. For heavy load condition, active power loss and OVSI value obtained by QOCNNA are 161.3266 kW and 29.0555 p.u., respectively. As a result, QOCNNA yields a significant enhancement in both two objective functions in comparison to NNA, ALO, and ISCA [25]. Moreover, standard deviations of optimal solutions found by QOCNNA are smaller than NNA and ALO, which shows QOCNNA

TABLE 9. Simulation results of QOCNNA for scenario 1 of 69-bus RDN.

Case study	Items	Load level		
		Light (0.5)	Nominal (1.0)	Heavy (1.6)
Initial case	Opened switches	69-70-71-72-73	69-70-71-72-73	69-70-71-72-73
	P_L (kW)	51.60	224.99	652.49
	V_{min} (p.u)	0.9567	0.9092	0.8445
Case 1	Opened switches	14-56-61-69-70	14-57-61-69-70	14-57-61-69-70
	P_L (kW)	23.6118	98.6046	267.1102
	PLR (%)	54.2446	56.1741	59.0634
	V_{min} (p.u)	0.9754	0.9495	0.9165
Case 2	Opened switches	69-70-71-72-73	69-70-71-72-73	69-70-71-72-73
	P_{DG}/(Bus) (MW)	0.1509/ (12) 0.1666/ (19) 0.8229/ (61)	0.2036/ (12) 0.3885/ (18) 1.6870/ (61)	0.5183/ (12) 0.4471/ (21) 2.6821/ (61)
	P_L (kW)	17.2558	70.6643	185.9060
	PLR (%)	66.5614	68.5925	71.5085
	V_{min} (p.u)	0.9878	0.9760	0.9597
Case 3	Opened switches	14-56-61-69-70	14-55-61-69-70	14-58-61-69-70
	P_{DG}/(Bus) (MW)	0.2079/ (12) 0.6963/ (61) 0.2364/ (64)	0.4181/ (12) 1.3805/ (61) 0.4827/ (64)	0.5920/ (12) 2.2781/ (61) 0.7698/ (64)
	P_L (kW)	8.6804	35.3683	92.6570
	PLR (%)	83.1790	84.2802	85.7996
	V_{min} (p.u)	0.9904	0.9802	0.9692

is also more robust than other methods in solving multi-objective SNR-DG problem.

Therefore, QOCNNA is a more robust and effective method than others in reducing active power loss and enhancing the OVSI of RDNs. Fig. 8 shows the convergence curves of QOCNNA and other methods for scenario 2 of 33-bus RDN at all load conditions. These figures show that QOCNNA obtains a faster convergence speed than NNA and ALO for all load conditions of this scenario.

From the obtained results, QOCNNA dominates the original NNA and other methods for solution accuracy and convergence rate in solving the SNR-DG problem for both scenarios of the 33-bus RDN. Therefore, QOBL and CLS are successfully integrated into QOCNNA to help the algorithm avoid local optimum trapping (exploration) and boost the convergence speed (exploitation) and hence improve QOCNNA performance.

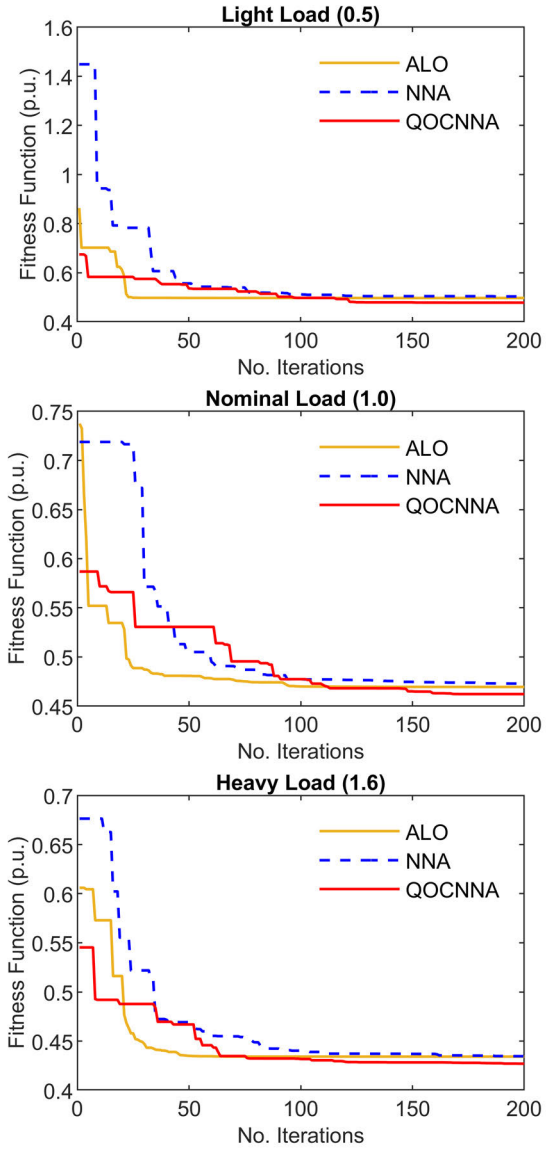

FIGURE 8. Convergence characteristics of QOCNNA, NNA and ALO for scenario 2 of 33-bus RDN.

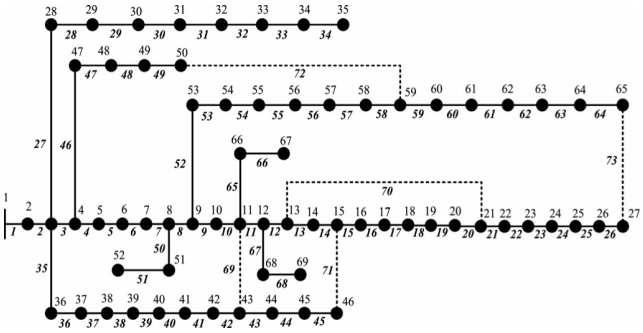

FIGURE 9. The IEEE 69-bus RDN.

B. 69-BUS RDN

The 69-bus RDN is a medium-scale system with a voltage level of 12.66 kV, 73 branches, 68 closed switches, and 5 opened switches [48]. Fig. 9 describes the single line diagram of 69-bus RDN. For base configuration, the total active and reactive loads of 69-bus RDN are 3.802 MW and 2.69 MVAr, respectively.

1) SCENARIO 1: ACTIVE POWER LOSS MINIMIZATION

Table 9 gives the simulation results found by the proposed QOCNNA for scenario 1 of 69-bus RDN. Figs. 10 and 11 depict active power losses and voltage profiles for all cases of scenario 1 of 69-bus RDN, respectively. For the light load condition, the initial power loss of the system is 51.60 kW, which is reduced to 23.6118 kW (case 1), 17.2558 kW (case 2), and 8.6804 kW (case 3), respectively. The

TABLE 10. Comparative results of QOCNNA and other methods for case 3 of scenario 1 of 69-bus RDN.

Load level	Methods	Opened switches	Sum P_{DG} (MW)	P_L (kW)	PLR (%)	Standard deviation
Light (0.5)	Initial case	69-70-71-72-73	-	51.60	-	-
	QOCNNA	14-56-61-69-70	1.1406	8.6804	83.1790	0.6475
	NNA	12-56-61-69-70	1.0333	9.6156	81.3667	0.7476
	ALO	9-13-56-64-70	1.1406	10.5353	79.5845	5.1837
	EOA [17]	12-55-62-69-70	0.970	9.4497	81.76	-
	IEOA [17]	12-55-62-69-70	1.098	9.03737	81.83	-
	ISCA [25]	12-17-57-62-69	0.9721	10.02	80.58	-
	HSA [26]	10-14-16-56-62	1.0021	11.07	78.55	-
	FWA [28]	13-56-63-69-70	0.9399	9.58	81.43	-
Nominal (1.0)	Initial case	69-70-71-72-73	-	224.99	-	-
	QOCNNA	14-55-61-69-70	2.2812	35.3683	84.2802	1.4818
	NNA	12-19-55-61-69	1.9751	39.1729	82.5892	1.5453
	ALO	9-13-20-53-62	2.2813	40.8180	81.8580	11.5016
	EOA [17]	12-18-56-63-69	2.263	37.5495	83.31	-
	IEOA [17]	10-13-57-61-70	1.831	36.3986	83.82	-
	ISCA [25]	12-19-57-63-69	1.8731	39.73	82.34	-
	HSA [26]	13-17-58-61-69	1.8718	40.3	82.08	-
	GA [26]	10-15-45-55-62	2.0292	46.5	73.38	-
	RGA [26]	10-14-16-55-62	2.0654	44.23	80.32	-
	FWA [28]	13-55-63-69-70	1.8181	39.25	82.55	-
	FF [33]	12-19-57-61-69	1.9371	40.3	82.08	-
Heavy (1.6)	Initial case	69-70-71-72-73	-	652.49	-	-
	QOCNNA	14-58-61-69-70	3.6399	92.6570	85.7996	5.8371
	NNA	12-18-58-63-69	3.5909	97.6747	85.0306	6.6672
	ALO	12-18-58-63-69	3.6500	99.4677	84.7558	40.9324
	EOA [17]	10-17-45-55-61	3.649	106.074	83.736	-
	IEOA [17]	10-12-13-57-62	3.649	100.4148	84.6	-
	ISCA [25]	14-55-62-69-70	2.7449	104.5	83.92	-
	HSA [26]	10-13-18-58-61	3.3828	104.67	83.96	-
	FWA [28]	13-57-63-69-70	2.9613	102.97	84.21	-

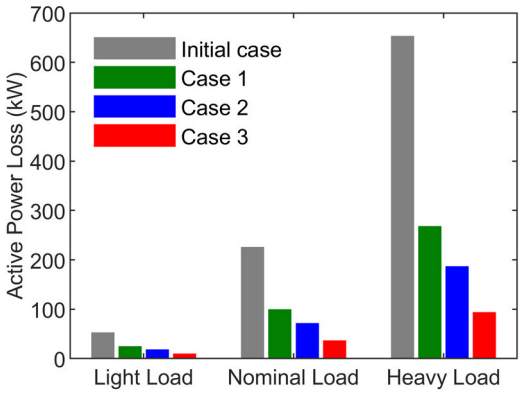

FIGURE 10. Active power loss for scenario 1 of 69-bus RDN at three load conditions.

corresponding PLR percentages are 54.2446%, 66.5614%, and 83.1790% for cases 1, 2, and 3. Similarly, at nominal and heavy load conditions, PLR related to cases 1, 2, and 3 are {56.1741%, 68.5925%, and 84.2802%} and {59.0634%, 71.5085%, and 85.7996%}, respectively.

According to the optimal results, PLRs in case 3 at all load conditions are the best values compared to cases 1 and 2. Furthermore, minimum voltage of the system for cases 1, 2, and 3 at light, nominal, and heavy load conditions are improved to {0.9754 p.u., 0.9878 p.u., and 0.9904 p.u.}, {0.9495 p.u., 0.9760 p.u., and 0.9802 p.u.}, and {0.9165 p.u., 0.9597 p.u., and 0.9692 p.u.}, respectively. The voltage profiles in case 3 are better improved than in other cases for all load conditions, as shown in Fig. 11. This implies the solution of SNR-DG is more effective than the ones of merely NR or DG in improving voltage issues of the 69-bus network.

Table 10 shows comparisons between QOCNNA and other methods at all load conditions for case 3 of scenario 1 of 69-bus RDN. At light load condition, QOCNNA defines the optimal NR with opened switches {14-56-61-69-70}, DG installations in 12^{th}, 61^{th}, and 64^{th} buses with respective DG sizes of 0.2079 MW, 0.6963 MW, and 0.2364 MW. The active power loss attained by QOCNNA is 8.6804 kW, whereas the ones obtained by NNA, ALO, EOA [17], IEOA [17], ISCA [25], HSA [26], and FWA [28], are 9.6156 kW, 10.5353 kW, 9.4497 kW, 9.03737 kW, 10.02 kW, 11.07 kW, and 9.58 kW, respectively. Accordingly, QOCNNA provides the lowest active power loss in comparison with other methods for this load condition. At normal load condition, opened switches obtained by QOCNNA are {14-55-61-69-70}. DGs are installed on 12^{th}, 61^{th}, and 64^{th} buses with 0.4181 MW, 1.3805 MW, and 0.4827 MW DG sizes. The active power loss achieved by QOCNNA for this case is the best result compared to other methods. At heavy load condition, QOCNNA offers the optimal NR with opened switches {14-58-61-69-70}, DG locations at 12^{th}, 61^{th}, and 64^{th} buses with respective DG sizes of 0.5920 MW, 2.2781 MW, and 0.7698 MW. The active power loss by QOCNNA (92.6570 kW) is lower than NNA

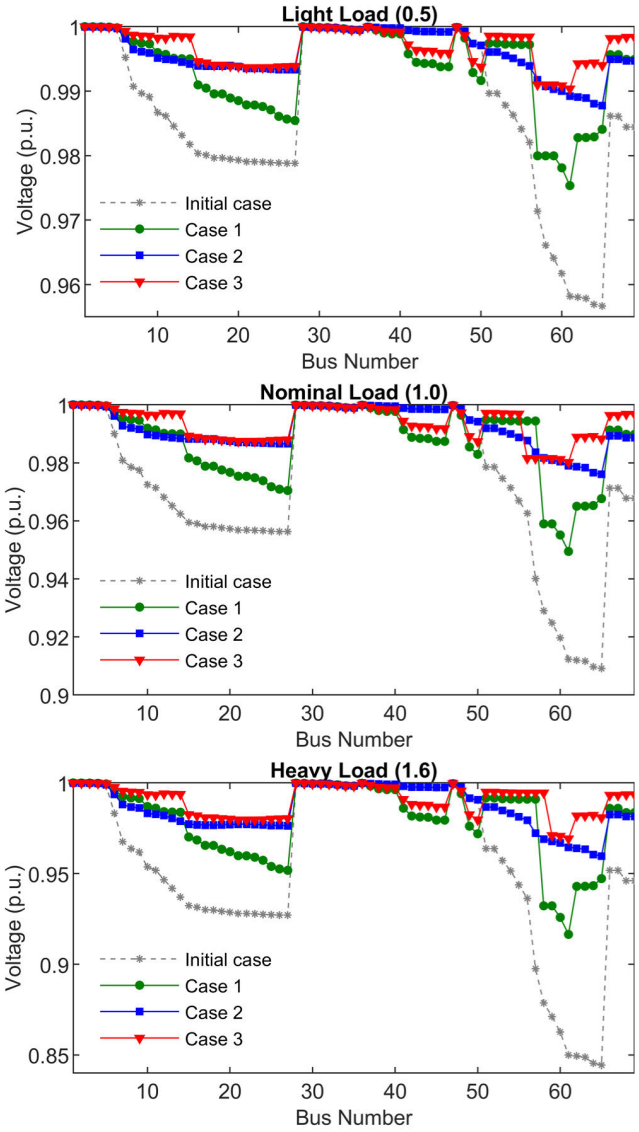

FIGURE 11. Voltage profiles for scenario 1 of 69-bus RDN at three load conditions.

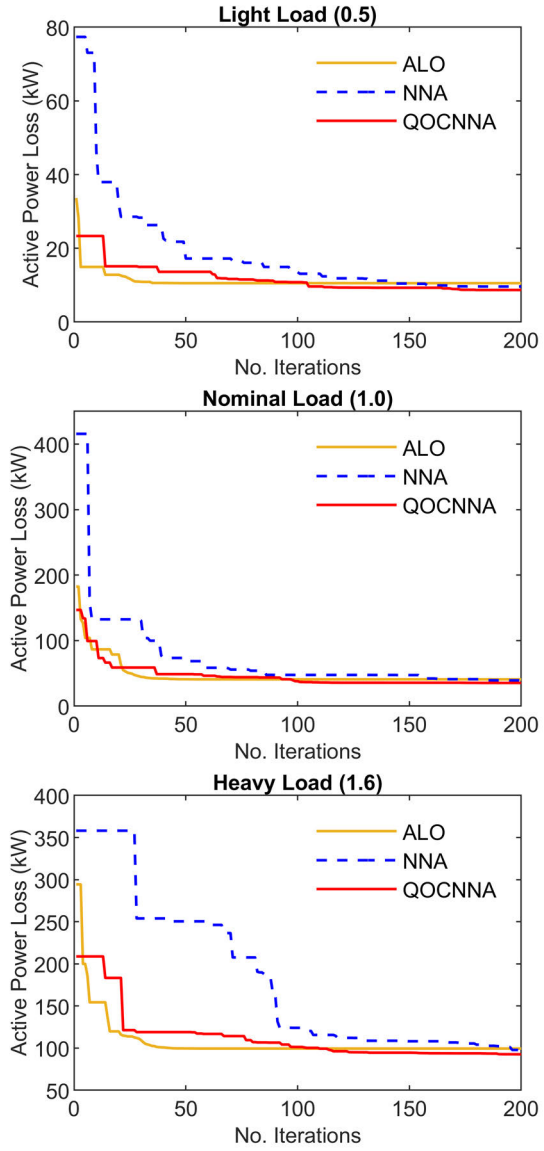

FIGURE 12. Convergence characteristics of QOCNNA, NNA and ALO for case 3 of scenario 1 of 69-bus RDN.

(97.6747 kW), ALO (99.4677 kW), EOA [17] (106.074 kW), IEOA [17] (100.4148 kW), ISCA [25] (104.5 kW), HSA [26] (104.67 kW), and FWA [28] (102.97 kW) for this load condition.

A comparative study in Table 10 shows that the proposed QOCNNA is an effective method for solving the SNR-DG problem. It is noted that QOCNNA is more robust than NNA and ALO in solving this scenario due to finding solutions with the lowest standard deviations for all load conditions. Fig. 12 portrays the convergence curves of QOCNNA, NNA, and ALO for scenario 1. From these figures, QOCNNA achieves better convergence than NNA and ALO for all case studies.

2) SCENARIO 2: ACTIVE POWER LOSS AND OVSI OPTIMIZATION

Multi-objective optimization of power loss minimization and voltage stability index maximization are investigated for the SNR-DG problem using QOCNNA in this scenario. Table 11 lists optimal results obtained by QOCNNA for this scenario. As for the consideration of active power loss and OVSI, the obtained PLRs are 82.7277%, 84.0223%, and 85.5659% for light, nominal and heavy loadings, respectively. Similarly, the OVSI values for the three loading conditions are effectively enhanced to 3.9261%, 8.5967% and 14.7118%, respectively. It is noted from the optimal results that SNR-DG application using QOCNNA shows a substantial improvement in both active power loss and OVSI objectives for all load conditions. Further, the voltage profile of the system is greatly enhanced after the SNR-DG as shown in Fig. 13. The minimum voltages are 0.9897 p.u., 0.9798 p.u., and 0.9668 p.u., respectively, for light, nominal and heavy load conditions after applying QOCNNA.

TABLE 11. Comparative results of QOCNNA and other methods for 69-bus RDN for scenario 2.

Load level	Method	Opened switches	P_{DG}/(Bus)	P_L (kW)	PLR (%)	OVSI	OVSI (%)	Fitness function	Standard deviation	V_{min} (p.u.)
Light (0.5)	Initial case	69-70-71-72-73	-	51.60	-	64.5966	-	-	-	0.9567
	QOCNNA	12-14-56-61-69	0.2046/ (66) 0.2730/ (27) 0.6630/ (61)	8.9133	82.7277	67.1327	3.9261	0.4096	0.0085	0.9897
	NNA	8-9-12-14-62	0.7333/ (61) 0.0666/ (68) 0.3401/ (24)	10.2143	80.2066	66.6881	3.2377	0.4291	0.0228	0.9890
	ALO	10-19-45-58-63	0.6888/ (61) 0.1346/ (68) 0.3173/ (24)	10.2016	80.2312	66.8867	3.5453	0.4281	0.0691	0.9890
	ISCA [25]	14-62-55-70-69	0.3593/ (60) 0.3015 (61) 0.4019 (65)	11.02	78.64	67.39	4.16	0.4370	-	0.9879
Nominal (1.0)	Initial case	69-70-71-72-73	-	224.99	-	-	-	-	-	0.9092
	QOCNNA	14-58-62-69-70	1.4113/ (61) 0.5167/ (27) 0.3533/ (12)	35.9485	84.0223	66.4800	8.5967	0.3881	0.0038	0.9798
	NNA	10-16-58-63-71	1.3893/ (61) 0.0549/ (46) 0.8371/ (21)	40.9018	81.8207	65.8789	7.6147	0.4060	0.0045	0.9772
	ALO	10-13-19-53-61	0.4549/ (67) 1.3808/ (61) 0.4456/ (64)	39.0790	82.6309	65.5967	7.1537	0.4016	0.0345	0.9789
	ISCA [25]	14-55-62-70-69	0.8100/ (60) 0.7978/ (61) 0.5738/ (65)	40	82.22	66.47	8.2	0.4007	-	0.9813
Heavy (1.6)	Initial case	69-70-71-72-73	-	652.49	-	-	-	-	-	0.8445
	QOCNNA	14-58-62-69-70	0.5723/ (12) 0.8300/ (27) 2.2477/ (61)	94.1823	85.5659	65.5707	14.7118	0.3626	0.0039	0.9668
	NNA	12-58-64-69-70	2.6447/ (61) 0.4971/ (21) 0.5082/ (66)	104.8400	83.9325	65.4932	14.5761	0.3743	0.0042	0.9599
	ALO	12-19-55-62-69	0.8500/ (27) 0.5312/ (51) 2.2688/ (61)	99.7307	84.7155	65.0262	13.7591	0.3707	0.0419	0.9672
	ISCA [25]	69-70-14-56-63	0.1061/ (60) 0.1108/ (61) 0.7720/ (65)	105.76	83.79	65.09	13.22	0.3769	-	0.9615

The results obtained by QOCNNA for scenario 2 of 69-bus RDN are compared to those obtained by other methods as presented in Table 11. For light load condition, QOCNNA obtains an active power loss of 8.9133 kW, which is lower than those of 10.2143 kW from NNA, 10.2016 kW from ALO, and 11.02 kW from ISCA [25]. Moreover, the OVSI values (in p.u.) achieved by QOCNNA, NNA, ALO, and ISCA [25] are 67.1327, 66.6881, 66.8867, and 67.39, respectively. QOCNNA obtains higher OVSI than NNA and ALO, and slightly lower than ISCA [25]. However, the fitness value of QOCNNA is the lowest compared to the other methods. From the simulated results, the best solution found by QOCNNA is better than those obtained by NNA, ALO, and ISCA [25] for two considered objectives.

Moreover, QOCNNA gives the lowest active power losses and the highest OVSI values in comparison to NNA, ALO, and ISCA [25] for nominal and heavy load conditions. As can be observed in Table 11, QOCNNA obtains the best fitness function values as compared to NNA and ALO for all load conditions. Hence, QOCNNA has a better performance than the other techniques in finding a compromise solution among the objective functions. The standard deviation values achieved by QOCNNA are also much lower than those achieved by NNA and ALO for all load levels, which confirms its robustness in solving the multi-objective SNR-DG problem.

Fig. 14 portrays the convergence characteristics of QOCNNA NNA, and ALO in terms of fitness function for three load conditions. It can be seen that QOCNNA can quickly converge to the minimum fitness value for all three load conditions. Generally, QOCNNA shows its superior performance over the original NNA and other methods in terms of solution accuracy and convergence speed in solving the SNR-DG problem of medium-scale 69-bus RDN.

C. 118-BUS RDN

The 118-bus RDN is a large-scale system with a voltage level of 11 kV, 132 branches, 118 closed switches, and 15 opened switches. For base configuration, the total active and reactive loads of 118-bus RDN are 22.709 MW and 17.041 MVAr, respectively.

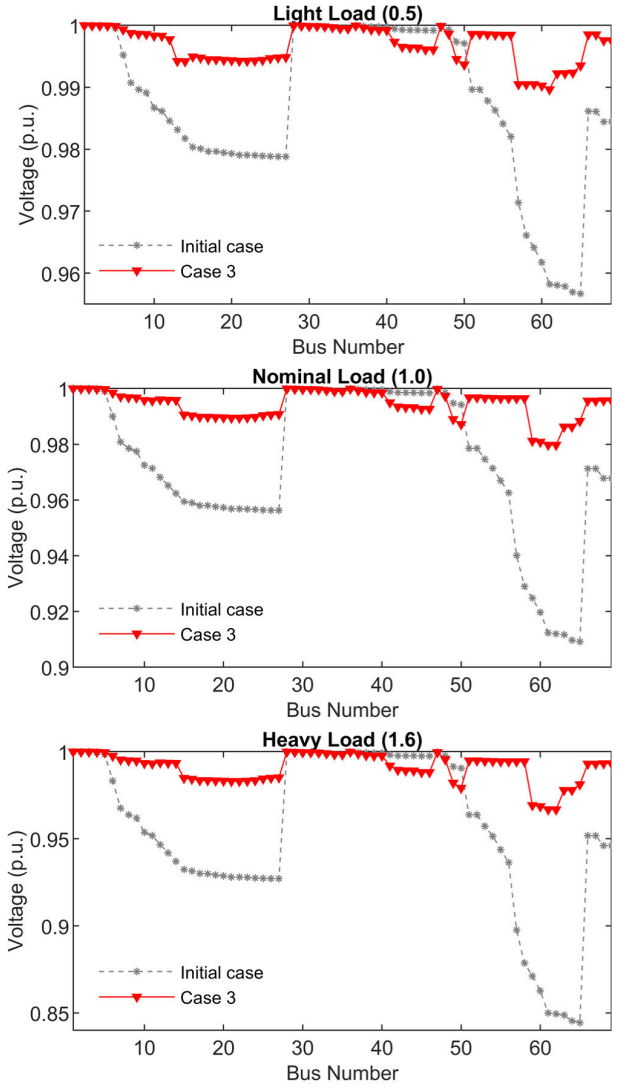

FIGURE 13. Voltage profiles for scenario 2 of 69-bus RDN at three load conditions.

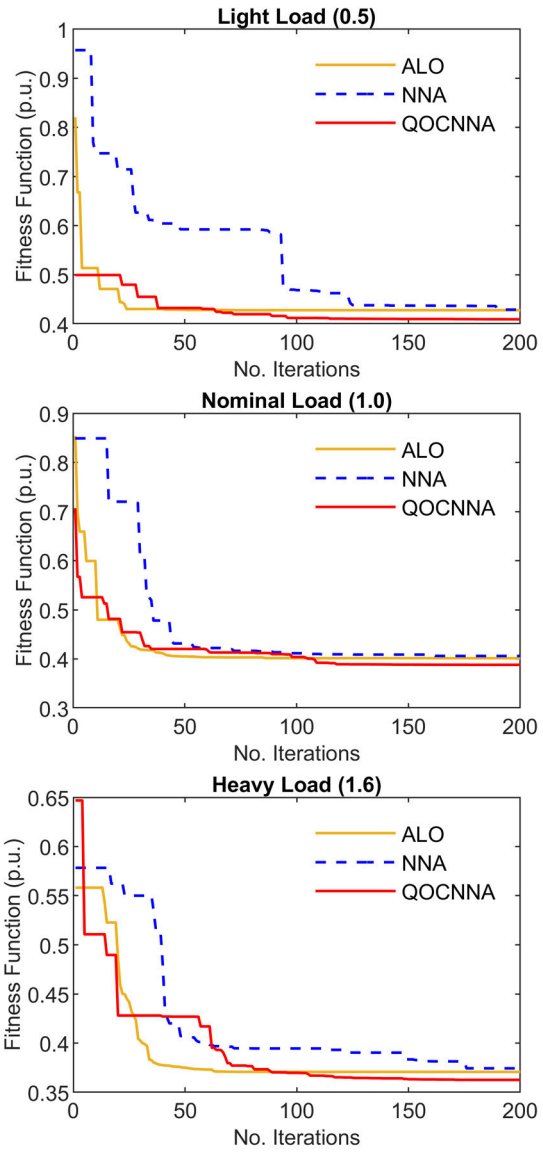

FIGURE 14. Convergence characteristics of QOCNNA, NNA and ALO for scenario 2 of 69-bus RDN.

1) SCENARIO 1: ACTIVE POWER LOSS MINIMIZATION

Similar to the above test systems, QOCNNA is also applied to 118-bus RDN for three cases at three load levels with the objective of active power loss minimization in this scenario. Simulation results are reported in Table 12. Figs. 15 and 16 portray active power losses and voltage profiles for all cases at three load conditions of 118-bus RDN, respectively.

In the initial case, the power losses at the light, nominal, and heavy load conditions are 297.15 kW, 1298.09 kW, and 3799.70 kW, respectively. Table 12 shows that the PLRs for cases 1 to 3 at light load condition are {31.4740%, 53.3198%, 54.2126%}, respectively. Meanwhile, at nominal and heavy load conditions, PLRs for cases 1, 2, and 3 are {34.2087%, 55.7169%, 59.9941%} and {38.7237%, 59.4512%, 63.8563%}, respectively. Moreover, the minimum voltage magnitudes are improved from 0.9385 p.u., 0.8688 p.u., and 0.7673 p.u. (initial case) to 0.9764 p.u., 0.9586 p.u., and 0.9384 p.u., respectively, at the light, nominal and heavy loading conditions in case 3. From the optimal results, case 3 reduces power loss and improves minimum voltage remarkably compared to cases 1 and 2 at all load conditions.

The result comparisons of QOCNNA, NNA, and ALO for case 3 of scenario 1 of 118-bus RDN are reported in Table 13. The convergence curves of QOCNNA, NNA and ALO are depicted in Fig. 17. Obviously, the performance of QOCNNA is better than those of NNA and ALO in terms of solution quality and convergence characteristics in all case studies. QOCNNA also obtains lower standard deviations than NNA and ALO, which demonstrates the robustness of QOCNNA over the two methods. Therefore, QOCNNA shows its effectiveness in solving the large-scale SNR-DG problem.

TABLE 12. Simulation results of QOCNNA for scenario 1 of 118-bus RDN.

Case study	Methods	Load level		
		Light (0.5)	Nominal (1.0)	Heavy (1.6)
Initial case	Opened switches	118-119-120-121-122-123-124-125-126-127-128-129-130-131-132	118-119-120-121-122-123-124-125-126-127-128-129-130-131-132	118-119-120-121-122-123-124-125-126-127-128-129-130-131-132
	P_L (kW)	297.15	1298.09	3799.70
	V_{min} (p.u)	0.9385	0.8688	0.7673
Case 1	Opened switches	23-25-34-39-42-50-58-71-74-95-97-109-121-129-130	23-25-34-39-42-50-58-71-74-95-97-109-121-129-130	23-25-34-39-42-50-58-71-74-95-97-109-121-129-130
	P_L (kW)	203.6241	854.0309	2328.3184
	PLR (%)	31.4740	34.2087	38.7237
	V_{min} (p.u)	0.9673	0.9323	0.8864
Case 2	Opened switches	118-119-120-121-122-123-124-125-126-127-128-129-130-131-132	118-119-120-121-122-123-124-125-126-127-128-129-130-131-132	118-119-120-121-122-123-124-125-126-127-128-129-130-131-132
	P_{DG}/(Bus) (MW)	1.4301/ (50) 1.1621/ (73) 1.0503/ (80) 0.8433/ (96) 1.4196/ (110)	2.8774/ (50) 2.3902/ (73) 2.1561/ (80) 1.6893/ (96) 3.1324/ (109)	4.6684/ (50) 4.2081/ (72) 3.4388/ (80) 2.5245/ (96) 4.7288/ (110)
	P_L (kW)	138.7097	574.8348	1540.7340
	PLR (%)	53.3198	55.7169	59.4512
	V_{min} (p.u)	0.9775	0.9540	0.9246
Case 3	Opened switches	11-23-38-42-53-58-70-117-122-125-127-128-129-130-132	16-21-33-39-43-51-60-70-109-121-125-127-128-129-130	22-26-33-39-42-52-58-70-121-125-126-128-129-130-131
	P_{DG}/(Bus) (MW)	1.9476/ (6) 1.3762/ (35) 0.2682/ (82) 1.8299/ (91) 1.3864/ (110)	4.6908/ (6) 2.1281/ (49) 3.3108/ (73) 1.5361/ (80) 1.8517/ (118)	3.0812/ (6) 3.7740/ (49) 4.9938/ (74) 2.9916/ (96) 4.9920/ (109)
	P_L (kW)	136.0566	519.3127	1373.3527
	PLR (%)	54.2126	59.9941	63.8563
	V_{min} (p.u)	0.9764	0.9586	0.9384

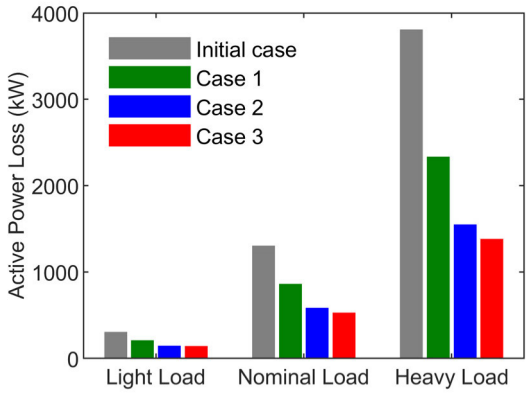

FIGURE 15. Active power loss for scenario 1 of 118-bus RDN at three load conditions.

2) SCENARIO 2: ACTIVE POWER LOSS AND OVSI OPTIMIZATION

In this scenario, the QOCNNA is applied to deal with the SNR-DG problem with the simultaneous optimization of

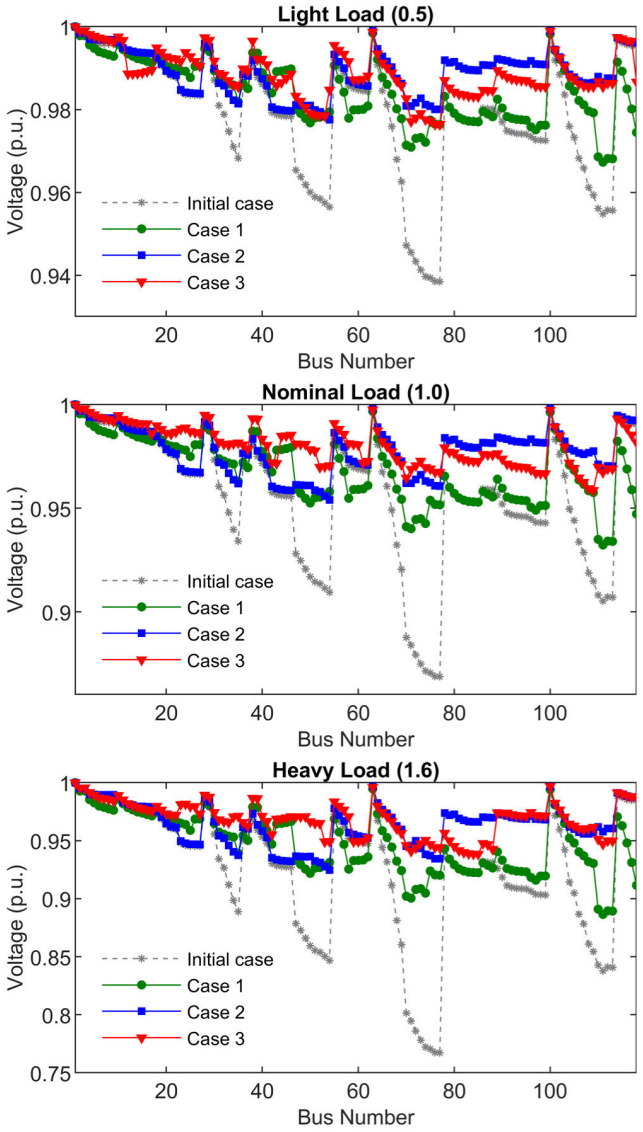

FIGURE 16. Voltage profiles for scenario 1 of 118-bus RDN at three load conditions.

active power loss and OVSI. Table 14 gives the optimal results for this scenario. From Table 14, QOCNNA not only obtains PLR of 56.8199%, 57.7960%, and 64.1986%, but it also enhances OVSI by 4.5563%, 10.1079%, and 18.7007% for light, nominal and heavy loadings, respectively. As depicted in Fig. 18, QOCNNA can effectively enhance the voltage profile of the system, with minimum voltages being improved to 0.9803 p.u., 0.9591 p.u., and 0.9345 p.u. for light, nominal and heavy loadings, respectively. It should be noted that the multi-objective SNR-DG problem on the 118-bus system is not documented in the literature and thus, comparing QOCNNA and previous studies is impossible. As seen in Table 14, the optimal solutions obtained by the QOCNNA for all load conditions are superior to those obtained by NNA and ALO for both active power loss and OVSI objectives. This proves that QOCNNA's performance is better than those

of NNA and ALO regarding the compromise among the two objective functions. The convergence characteristics shown in Fig. 19 demonstrate the excellent global search ability of the QOCNNA compared with NNA and ALO. Moreover, the standard deviation of solutions found by the QOCNNA is also the smallest among compared algorithms for all load conditions of this scenario.

Hence, QOCNNA can effectively solve the SNR-DG problem with a high-quality solution. The good performance of QOCNNA is due to the incorporation of two search strategies including CLS and QOBL. In QOCNNA, the QOBL approach is integrated to explore a more promising region; meanwhile, the CLS approach is used to locally exploit the neighborhood of the best solutions to enhance the solution accuracy. These approaches improve the exploration and exploitation capabilities of QOCNNA to avoid premature convergence and local optima stuck. Hence, QOCNNA can find the optimal solution with a faster convergence speed.

The QOCNNA, NNA, and ALO are implemented on a 2.6 GHz 4-core computer with 16 GB of RAM. Table 15 reports the average computational times of QOCNNA, NNA, and ALO for each case. Computational times of QOCNNA are longer than NNA and ALO for most case studies. However, QOCNNA has faster computational time than ALO for all cases of 118-bus large-scale system. The long computational speed of QOCNNA is due to the extra search time of QOBL and CLS strategies. Although QOCNNA does not dominate the computational time over NNA and ALO, QOCNNA outperforms the two methods for the solution quality, convergence characteristic, and robustness in all cases.

D. EXAMINATION OF DAILY LOAD AND GENERATION VARIATIONS ON NR AND DG ALLOCATION PROBLEM

From the above simulated results of three separate loading levels, the optimal solution of open switches, locations and sizes of DGs varies considerably in relation to different loading conditions. Therefore, the problem is to determine the optimal network configuration and settings of DGs when the actual load changes daily. To address this, a novel methodology has been developed for finding the optimal opened switches, locations, and sizes of DGs based on a load demand curve of a typical day.

Recalling that the object function of minimization of operational cost (Co) in RDN usually comprises two factors, i.e., the cost of shifting switches (Co_b) and the cost of active power loss as follows:

$$Co = n_s \times Co_b + Co_a \times \sum_{k=1}^{n_s} P_{loss,k} \times T_k \tag{33}$$

where Co_a is energy price; n_s is the number of times shifting switches; T_k is operating time of configuration k and $P_{loss,k}$ is active power loss induced by configuration k.

However, some practical RDNs whose cost of shifting switches is too large when compared with the savings from power loss reduction. Also, the system of supervisory control and data acquisition has not been suitably developed yet, leading to the switches cannot be controlled remotely. Accordingly, the process of shifting the status of switches will result in a power outage since in this process, power from a path delivered to loads is first cut and power is then supplied to loads via another path. Hence, in this situation the switches will be remained unchanged for a long time by power suppliers and the prime objective of the NR process is therefore minimizing the cost of energy loss during variable load period. In other words, the problem of minimization of the operational cost will be converted into the problem of finding a constant network configuration during the operating time so as to minimize energy loss. The object function of the NR problem for minimizing energy loss (EL) can be stated as

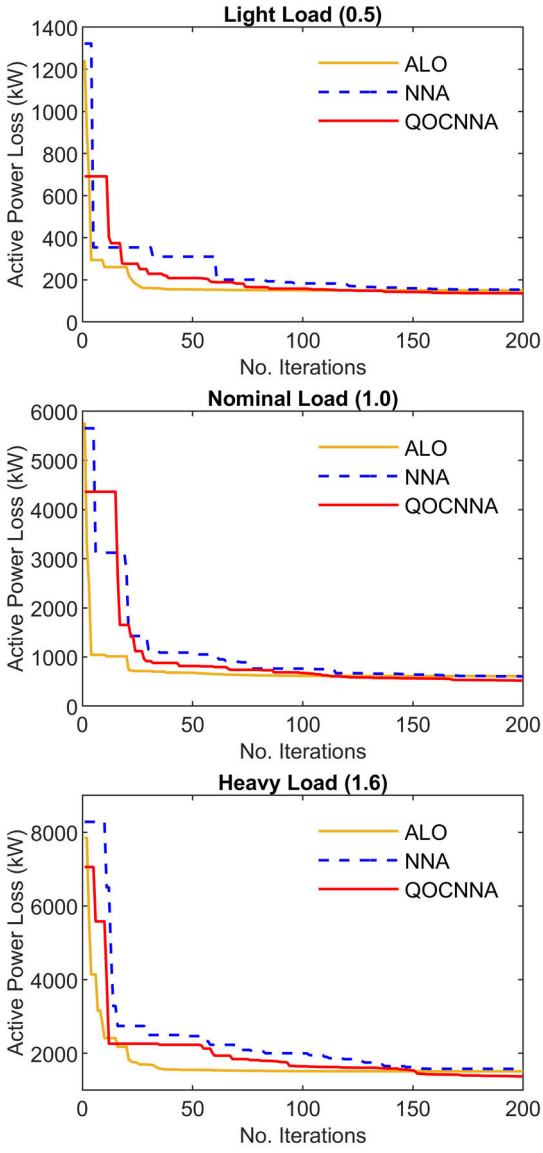

FIGURE 17. Convergence characteristics of QOCNNA, NNA and ALO for case 3 of scenario 1 of 118-bus RDN.

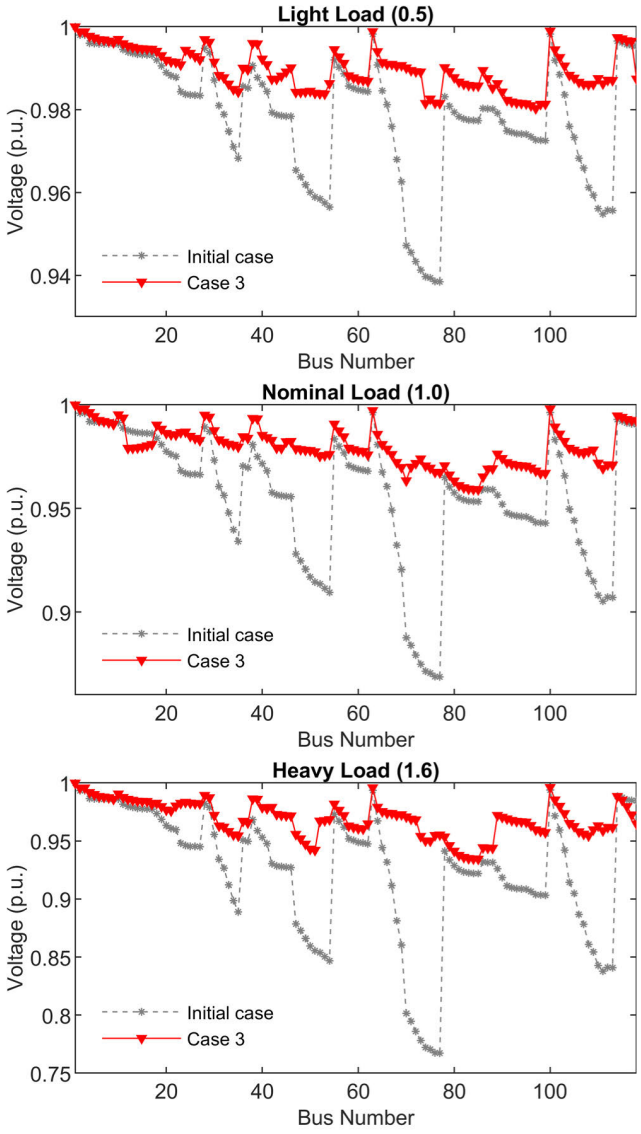

FIGURE 18. Voltage profiles for scenario 2 of 118-bus RDN at three load conditions.

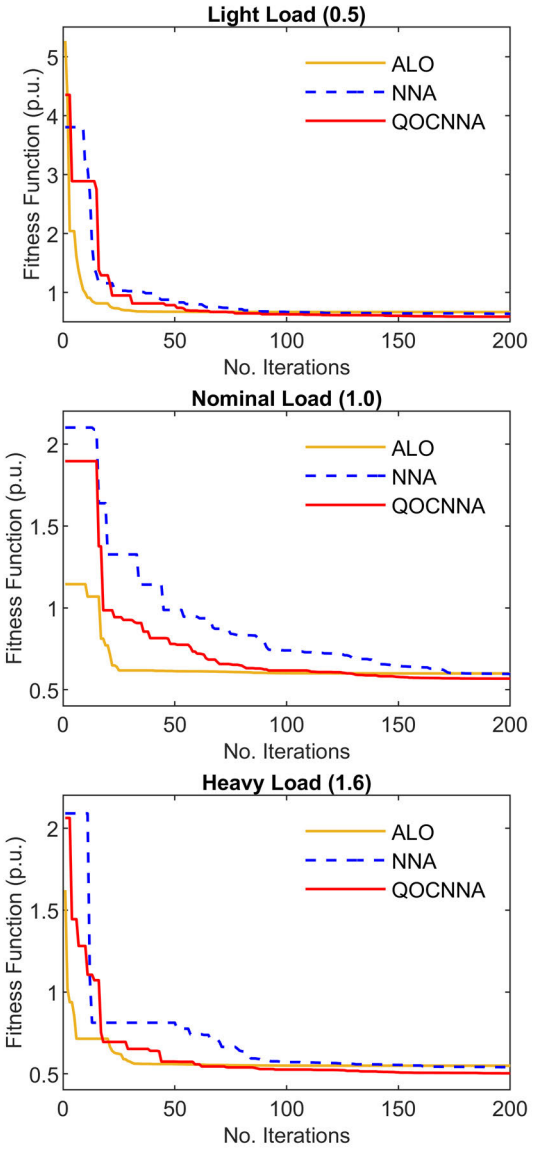

FIGURE 19. Convergence characteristics of QOCNNA, NNA and ALO for scenario 2 of 118-bus RDN.

follows:

$$EL(S) = \sum_{t=1}^{24} P_{loss}(t) \times \Delta t \tag{34}$$

Besides network reconfiguration, the allocation of photovoltaic (PV)-based DG has also been examined on the scenario of daily variable loads for minimizing energy loss. In this scenario, one PV DG is considered for allocation where the outputs of PV DG are estimated from the average output curve as in Fig. 20 [40]. Fig. 21 illustrates an hourly load demand curve of the 69-bus network which is similar to the one in [40]. To make a fair and efficient comparison with the analytical method in [40] for the case of only PV DG, the object function *EL* has been modified for computing total annual energy loss (*AEL*) with an interval Δt of 1 h. Precisely, the computation of *AEL* is the summation of the active power losses of 24 loading levels over a day times 365 days a year. In addition, this object function has also been adopted to investigate two remaining cases including the case of only NR and the case of simultaneous NR and PV DG allocation. For the general case of simultaneous optimization, the function *AEL* may be expressed as:

$$AEL(S, L, P, Q) = 365 \times \sum_{t=1}^{24} P_{loss}(t) \times \Delta t \tag{35}$$

For the test network, only is the 69-bus RDN with medium-size selected for the investigations. Bus voltage profile of the 69-bus network in a representative day before the optimization is illustrated in Fig. 22. To validate the simulation results of the proposed QOCNNA for case studies, we have further run four different optimization methods including whale optimization algorithm – WOA [38], sine cosine algorithm

TABLE 13. Comparative results of QOCNNA and other methods for case 3 of scenario 1 of 118-bus RDN.

Load level	Method	Opened switches	Sum P_{DG} (MW)	P_L (kW)	PLR (%)	Standard deviation
Light (0.5)	Initial case	118-119-120-121-122-123-124-125-126-127-128-129-130-131-132	-	297.15	-	-
	QOCNNA	11-23-38-42-53-58-70-117-122-125-127-128-129-130-132	6.8083	136.0566	54.2126	16.4666
	NNA	8-12-23-34-43-61-71-74-87-95-121-122-129-130-131	6.6678	153.1411	48.4631	19.7526
	ALO	11-21-32-39-42-43-50-55-60-66-108-127-128-129-130	6.1750	149.8976	49.5547	33.5727
Nominal (1.0)	Initial case	118-119-120-121-122-123-124-125-126-127-128-129-130-131-132	-	1298.09	-	-
	QOCNNA	16-21-33-39-43-51-60-70-109-121-125-127-128-129-130	13.5176	519.3127	59.9941	63.4359
	NNA	12-22-39-43-58-70-76-109-121-122-125-126-129-130-132	13.4878	605.1948	53.3781	88.1335
	ALO	26-39-45-52-59-71-82-98-120-121-125-126-130-131-132	10.1101	611.3221	52.9061	90.7589
Heavy (1.6)	Initial case	118-119-120-121-122-123-124-125-126-127-128-129-130-131-132	-	3799.70	-	-
	QOCNNA	22-26-33-39-42-52-58-70-121-125-126-128-129-130-131	19.8326	1373.3527	63.8563	134.5878
	NNA	22-39-51-61-70-82-97-118-119-121-125-126-130-131-132	19.7210	1580.4894	58.4049	146.3508
	ALO	23-25-34-39-45-50-61-69-98-107-109-123-125-127-130	16.9254	1512.6655	60.1899	193.5097

– SCA [39], ALO [37], and original NNA [36] methods for each case study to compare results. The algorithm parameters of WOA, SCA, ALO and NNA are set the same as in their original studies [36]–[39]. The respective optimization results for the three cases of NR and PV DG allocation with the aim of minimizing the function *AEL* in the 69-bus network are tabulated in Table 16 in which the step-by-step computation procedure in Appendix A is utilized.

For the case of only NR, the proposed QOCNNA obtains an optimal configuration with opened switches {14-57-63-69-70}, which is fixed during varying of loads. Hourly active power losses relative to this configuration are depicted in Fig. 23. This configuration achieves a reduced *AEL* value of 617.69 MWh compared with an initial *AEL* value of 1,381.97 MWh. Notably, this value is significantly lower than 760.65 MWh from WOA [38], 784.04 MWh from SCA [39], 790.06 MWh from ALO [37], and 738.60 MWh from NNA. Accordingly, the QOCNNA obtains the highest cost savings of 91,713.84 $ among the comparative optimizers. Also, the QOCNNA requires a CPU time of approximately 147.93 s to reach the final solution, which is faster than WOA and ALO, but slower than SCA and NNA. QOCNNA has a longer CPU time due to the extra time relative to the exploration process of QOBL and the exploitation process of CLS as well. It is noted that the extra search time makes a remarkable improvement in the performance of QOCNNA. Further, the voltage profiles of the network in a representative day after NR are plotted in Fig. 24. From the figure, the optimal solution of NR leads to a significant improvement in voltage magnitude at all buses compared with the initial case shown in Fig. 22. Convergence curves of five methods for minimizing the *AEL* function in Case 1 are depicted in Fig. 25. The QOCNNA shows a fast convergence to the optimal solution within 27 iterations while the remaining methods fail to approach the optimal solution. To further analyze the convergence of NNA, in the first iterations with a sufficiently large modification factor (MF), the bias operator will be more likely activated to satisfy the exploration ability of NNA. This likelihood will gradually decrease as the MF decreases by iterations, meaning that in later iterations the transfer function operator may be activated to help NNA implement the local search in the designed space. In fact, with a decreasing step of 0.01, a MF value of 0.5 reached at the 50^{th} iteration is large enough for NNA to remain the exploration ability throughout the searching process. This causes an over exploration situation without effective exploitation, resulting in the NNA being trapped in a local minimum for this case. Meanwhile, the exploitation ability of QOCNNA has been significantly upgraded, which leads to its convergence speed boosted in the first iterations thanks to CLS integration. Besides, the combined QOBL strategy has assisted QOCNNA to a better balance between the exploration and exploitation during the searching process.

For the case of only PV DG, the proposed QOCNNA achieves a final solution with the bus location of 61 and maximum size of 2.304 MVA for one PV DG connection into the 69-bus network. With this connection, the *AEL* value of the network is improved to 569.78 MWh from 1,381.97 MWh in the initial case (i.e. 58.77 % reduction) and the respective cost savings is 97,462.83 $. Clearly, the *AEL* obtained by QOCNNA is the lowest compared with those of analytical method (AM) [40], exhaustive load flow (ELF) [40], WOA [38], SCA [39], ALO [37], and NNA. Also, the execution time of

TABLE 14. Comparative results of QOCNNA and other methods for 118-bus RDN for scenario 2.

Load level	Method	Opened switches	P_{DG}/(Bus)	P_L (kW)	PLR (%)	OVSI	OVSI (%)	Fitness function	Standard deviation	V_{min} (p.u)
Light (0.5)	Initial case	118-119-120-121-122-123-124-125-126-127-128-129-130-131-132	-	297.15	-	107.3935	-	-	-	0.9385
	QOCNNA	23-39-42-53-73-97-117-119-122-123-125-126-129-130-132	1.2344/(50) 0.8467/(70) 1.3549/(7) 1.4211/(110) 1.7181/ (86)	128.3092	56.8199	112.2867	4.5563	0.5892	0.0227	0.9803
	NNA	21-39-42-53-59-71-82-109-119-122-125-126-127-130-132	1.1881/(50) 0.0229/(7) 1.1213/(24) 0.9181/(118) 1.6784/(97)	148.9972	49.8577	111.8196	4.1213	0.6391	0.0288	0.9738
	ALO	11-23-34-37-44-53-72-122-123-125-126-128-129-130-131	1.0231/(96) 0.9456/(110) 0.7224/(102) 0.5972/(107) 1.2467/(75)	160.9496	45.8353	111.2229	3.5657	0.6688	0.3950	0.9704
Nominal (1.0)	Initial case	118-119-120-121-122-123-124-125-126-127-128-129-130-131-132	-	1298.09	-	98.019	-	-	-	0.8688
	QOCNNA	1-22-34-39-44-51-61-70-86-97-123-125-129-130-131	3.5988/(73) 3.1723/(109) 1.7116/(42) 1.9153/(50) 3.2229/(4)	547.8465	57.7960	107.9267	10.1079	0.5679	0.0279	0.9591
	NNA	21-26-37-42-51-59-69-76-107-109-119-125-127-130-132	2.0913/(50) 0.0120/(72) 3.8720/(73) 3.1697/(80) 3.0775/(37)	596.0247	54.0845	107.2264	9.3934	0.5956	0.0355	0.9329
	ALO	11-23-39-41-50-57-61-73-104-107-109-122-126-127-132	1.3689/(71) 1.8395/(43) 3.5469/(97) 1.9234/(118) 4.3768/(79)	603.1019	53.5393	107.1996	9.3661	0.5995	0.1508	0.9396
Heavy (1.6)	Initial case	118-119-120-121-122-123-124-125-126-127-128-129-130-131-132	-	3799.7	-	86.9977		-	-	0.7673
	QOCNNA	16-21-39-51-61-72-75-108-118-122-125-127-129-130-132	4.5698/(47) 3.9386/(110) 5.0000/(91) 2.6058/(70) 3.1126/(42)	1360.3474	64.1986	103.2669	18.7007	0.5033	0.0275	0.9345
	NNA	6-22-24-42-51-61-70-85-121-125-127-128-129-131-132	5.0000/(109) 4.0418/(49) 2.7618/(8) 4.9957/(11) 5.0000/(73)	1538.8802	59.5000	101.3394	16.4851	0.5410	0.0347	0.9362
	ALO	21-26-34-39-44-52-59-76-85-116-121-125-126-127-129	4.4225/(72) 3.6669/(50) 4.1493/(79) 2.5103/(118) 3.8367/(107)	1599.9892	57.8917	102.3773	17.6781	0.5497	0.0618	0.9281

QOCNNA is longer than AM [40], WOA [38], SCA [39], ALO [37], and NNA except for ELF [40]. It is reasonable when QOCNNA takes much more time than NNA to find a solution due to extensive search strategies. Further, the hourly optimized outputs of PV DG related to the daily load demand of the 69-bus network by using different optimizers are plotted in Fig. 26. The hourly active power losses of the network obtained by the methods before and after the PV DG connection are shown in Fig. 27. From the two figures, in the time range of 6 – 20 hours when network load demand tends to increase, the output of PV DG optimized by QOCNNA meets the load demand better than those optimized by the

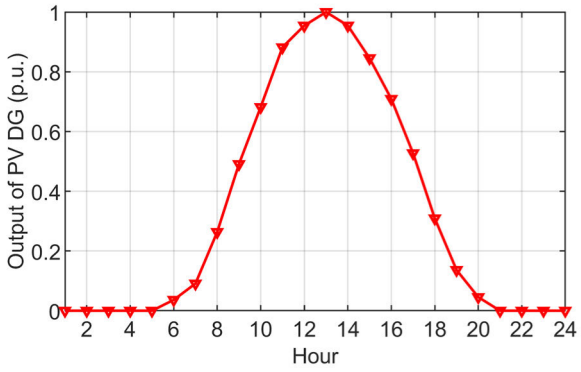

FIGURE 20. Hourly power output of PV DG in a representative day.

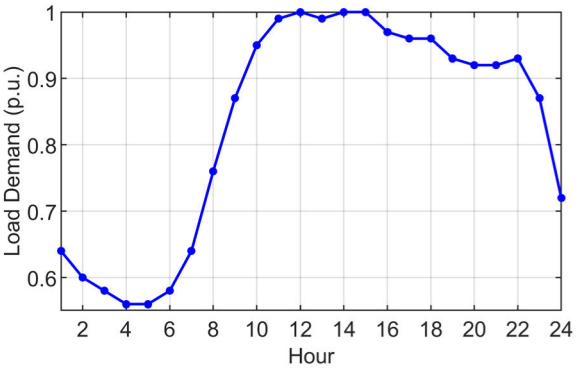

FIGURE 21. Hourly load demand of network in a representative day.

rest of methods. This leads to lower power loss values in this period achieved by QOCNNA. In addition, the voltage profiles of the network in a representative day after connecting one PV DG at bus 61 are plotted in Fig. 28. From the figures 22 and 28, for hours with non-zero outputs of PV DG, the voltage profiles at nodes from 53 to 65 of the feeder where PV DG connected is remarkably improved. Moreover, convergence curves of five methods in solving the PV DG-only case of the network are shown in Fig. 29. The three ALO, NNA and QOCNNA methods have high competition in exploring the search space and the QOCNNA exhibits a strong search ability to approach the best solution among the three. For the convergence of NNA, in the first 50 iterations when the MF decreases from 1 to 0.5 by a step of 0.01, the MF values belonging to this range are large enough to activate the bias operator with a high probability for performing the exploration. In this phase, there are relatively large changes in the convergence curve. In later iterations, once the MF decreases to sufficiently small values, it is highly likely that the transfer function operator will be activated to execute the exploitation. Due to the local search at this stage, there are small changes observed in the convergence curve. For QOCNNA, thanks to the integrated CLS strategy, the exploitation aspect is noticeably enhanced in the first 50 iterations which leads to a better convergence profile as compared with NNA. In addition, the use of the QOBL strategy also supports QOCNNA for the exploration ability in the later iterations,

TABLE 15. Comparisons of QOCNNA and other methods for computational time in seconds.

System	Scenario	Load level	QOCNNA	NNA	ALO
33-bus	1	Light	34.4241	21.1106	34.6392
		Nominal	33.7666	21.3928	33.1026
		Heavy	33.6635	22.7201	30.1585
	2	Light	34.9202	23.7738	30.1680
		Nominal	35.4668	24.1679	30.7914
		Heavy	37.0243	24.9710	31.4698
69-bus	1	Light	40.9544	25.7319	37.4283
		Nominal	40.6161	26.4172	37.2397
		Heavy	44.0282	28.3895	36.1827
	2	Light	41.9397	28.8032	35.6665
		Nominal	43.3064	30.2412	36.4542
		Heavy	46.8053	32.6261	35.3223
118-bus	1	Light	57.8684	36.6683	83.8207
		Nominal	61.8395	42.8737	84.9837
		Heavy	68.3257	47.8329	91.0057
	2	Light	58.2855	52.1114	86.3282
		Nominal	64.8470	56.1389	89.3360
		Heavy	69.5089	63.0611	91.5608

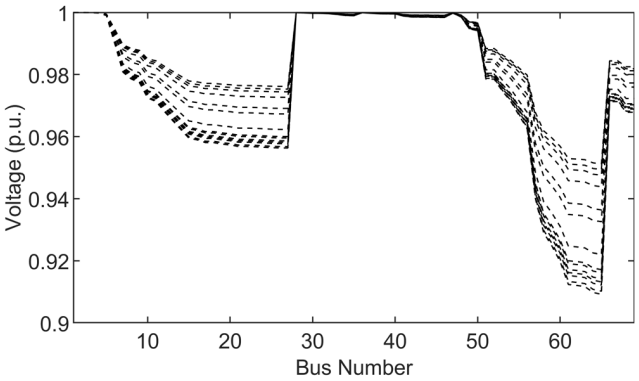

FIGURE 22. Voltage profile of 69-bus RDN in a representative day before optimization.

resulting in a better convergence tend observed. Clearly, the QOCNNA with integrated improvement strategies shows a faster convergence speed and higher solution accuracy for this case. This proves that QOCNNA achieves a better trade-off between the exploration and exploitation properties as compared with NNA. While the WOA and SCA methods fail to achieve an optimal solution for this case, showing a weak search capability.

Concerning the practical case of simultaneous NR and PV DG allocation, the QOCNNA settles at the optimal solution with the opened switches of {16-56-64-69-71} and the connection of one PV DG at bus 61 with a maximum size of 2.113 MVA, which results in a reduced *AEL* value of 369.08 MWh (i.e. 73.29% reduction). This *AEL* value is the lowest among those found by WOA, SCA, ALO and NNA methods. It means the highest cost savings of 121,547.10 $ is achieved by QOCNNA. Regarding CPU time, QOCNNA requires about 1012.16 s for the optimization process. Although it takes more time than the remaining methods, its solution quality is remarkably better. Also, the hourly

TABLE 16. Results of NR and PV DG allocation for daily variable load and generation scenario using different optimizers.

Case study	Methods	Opened switches	S_{DG}/(Bus)	Optimal *pf*	Annual energy loss before optimization (MWh)	Annual energy loss after optimization (MWh)	Annual energy loss mitigation (%)	Cost savings[b] ($)	Avg. CPU time
Case 1 – Only NR	QOCNNA	14-57-63-69-70	-	-	1381.97	**617.69**[a]	55.30	91,713.84	147.93
	NNA	5-11-55-62-70	-	-	1381.97	738.60	46.55	77,204.91	65.17
	ALO	56-63-69-70-71	-	-	1381.97	790.06	42.83	71,029.20	180.45
	WOA	20-42-44-56-63	-	-	1381.97	760.65	44.95	74,558.56	151.78
	SCA	5-14-15-53-62	-	-	1381.97	784.04	43.26	71,751.44	82.39
Case 2 – Only PVDG	QOCNNA	-	2.304/(61)	0.783	1381.97	**569.78**	58.77	97,462.83	1524.85
	NNA	-	2.446/(61)	0.807	1381.97	578.90	58.11	96,368.62	971.52
	ALO	-	2.361/(61)	0.801	1381.97	599.31	56.63	93,919.82	744.30
	WOA	-	3.498/(61)	0.86	1381.97	698.13	49.48	82,061.40	698.62
	SCA	-	2.661/(61)	0.857	1381.97	910.01	34.15	56,635.02	994.51
	AM [40]	-	3.618/(61)	0.83	1381.97	657.72	52.40	86,910.00	0.10
	ELF [40]	-	2.985/(61)	0.82	1381.97	608.81	55.94	92,779.20	>1625.6
Case 3 – NR-PVDG	QOCNNA	16-56-64-69-71	2.113/(61)	0.784	1381.97	**369.08**	73.29	121,547.10	1012.16
	NNA	9-14-56-64-70	2.876/(61)	0.938	1381.97	454.07	67.14	111,347.93	571.7
	ALO	14-56-64-69-71	2.984/(61)	0.872	1381.97	422.92	69.39	115,086.73	753.22
	WOA	12-63-69-70-72	3.414/(61)	0.925	1381.97	707.19	48.82	80,973.98	661.31
	SCA	9-15-56-62-71	0.391/(61)	0.875	1381.97	703.06	49.12	81,469.82	387.75

pf denotes power factor of DG; [a]The lowest object value is in bold; [b]Tariff covers 0.12 $/kWh and cost savings in $ is equal to $(AEL_{before} - AEL_{after}) \times 10^3 \times 0.12$.

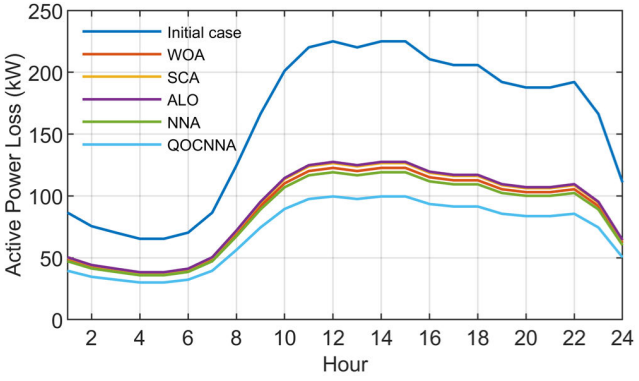

FIGURE 23. Hourly power loss of 69-bus RDN before and after NR using different optimizers.

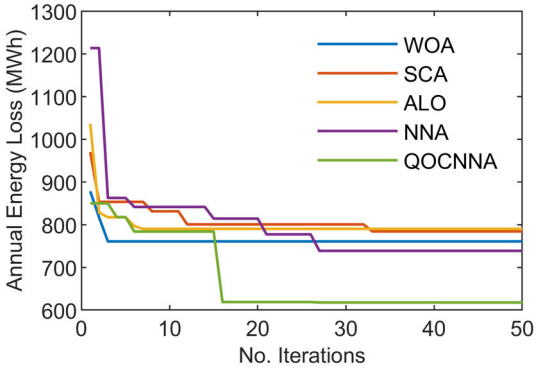

FIGURE 25. Convergence characteristics of optimization methods for annual energy loss minimization in Case 1 of 69-bus RDN.

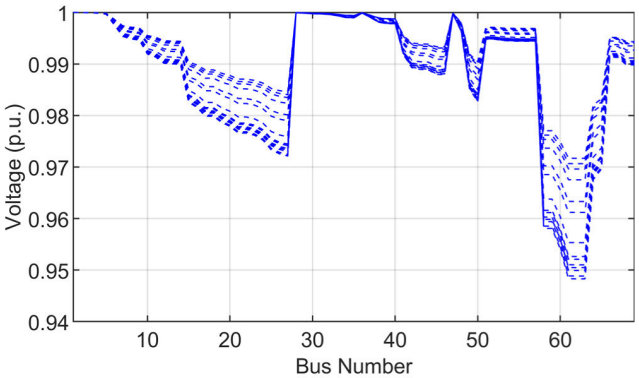

FIGURE 24. Variation of voltage profiles of 69-bus RDN in a typical day for Case 1 using QOCNNA.

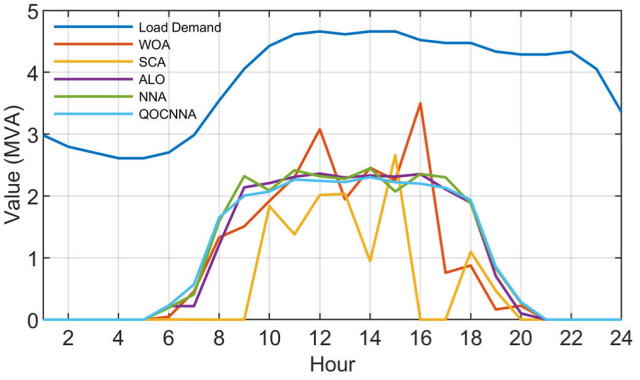

FIGURE 26. Comparison of daily load demand and respective optimal outputs of PVDG in Case 2 using different optimizers.

optimized outputs of PV DG associated with the daily load demand of the network using other methods are depicted as in Fig. 30. The hourly active power losses of the network obtained by the methods before and after simultaneous NR and PV DG allocation are shown in Fig. 31. The combination of NR and PV DG allocation results in a more significant reduction in power loss at the hours of zero output of PV

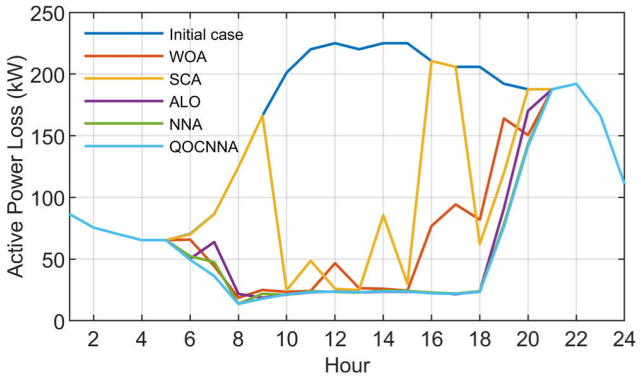

FIGURE 27. Hourly power loss of 69-bus RDN in Case 2 using different optimizers.

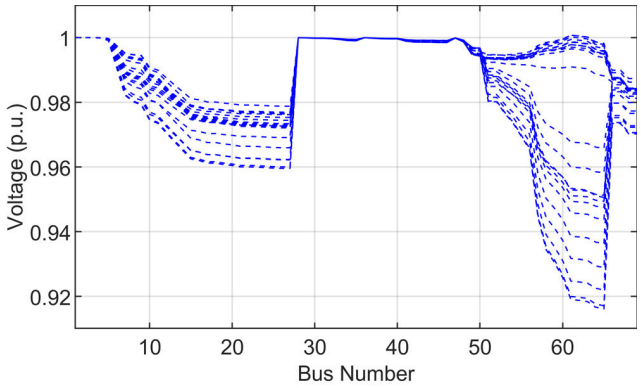

FIGURE 28. Variation of voltage profiles of 69-bus RDN in a typical day for Case 2 using proposed QOCNNA.

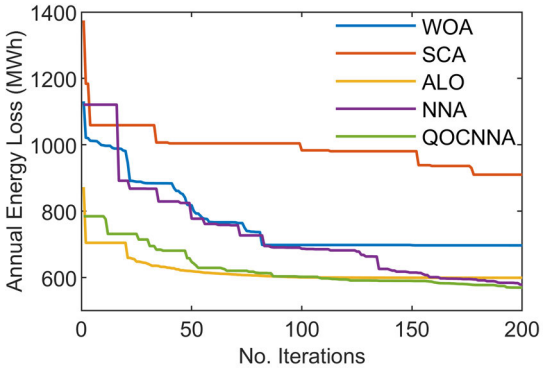

FIGURE 29. Convergence characteristics of optimization methods for annual energy loss minimization in Case 2 of 69-bus RDN.

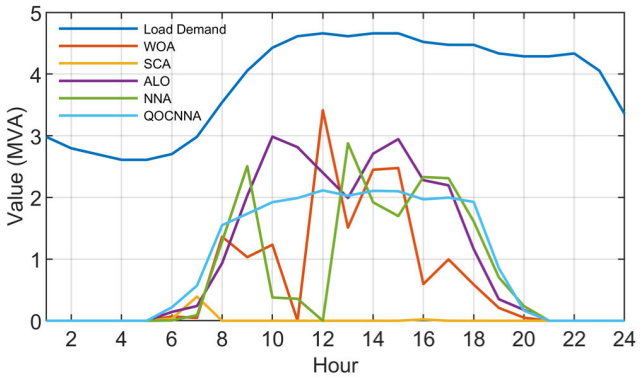

FIGURE 30. Comparison of daily load demand and respective optimal outputs of PV DG in Case 3 using different optimizers.

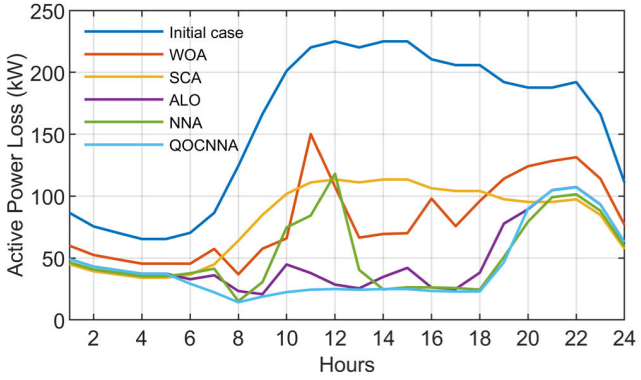

FIGURE 31. Hourly power loss of 69-bus RDN in Case 3 using different optimizers.

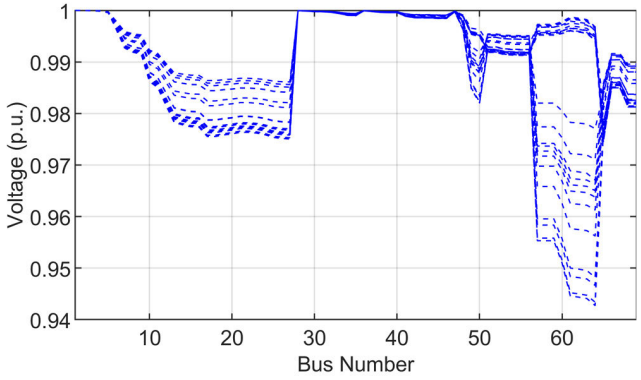

FIGURE 32. Variation of voltage profiles of 69-bus RDN in a typical day for Case 3 using QOCNNA.

DG as compared with the solution of only PV DG allocation in Fig. 27. Moreover, most of the hourly power loss values obtained by QOCNNA are lower than those obtained by the comparative methods. Further, the voltage profiles of the network in a representative day after simultaneous NR and PV DG allocation are plotted in Fig. 32. The simultaneous solution of NR and PV DG leads to a significant improvement in voltage magnitude at all buses compared with the initial case shown in Fig. 22. Finally, convergence curves of the applied methods for minimizing *AEL* function in this case are illustrated in Fig. 33. The QOCNNA along with the ALO and NNA again shows high competition in the solution search process in this case and the QOCNNA is the unique method converging to the optimal solution. Compared with NNA, QOCNNA always shows the ability to search in the area of higher quality solutions and approaches the optimal solution with a faster convergence rate. This proves that the improvement strategies have helped QOCNNA achieve better

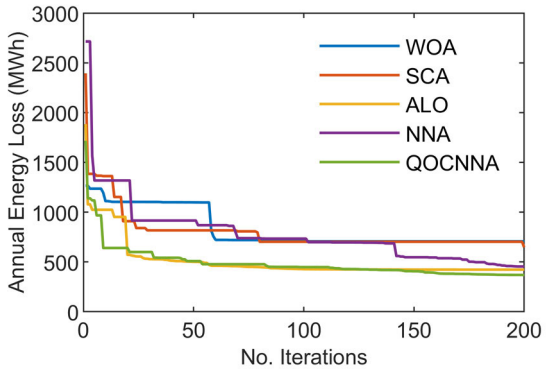

FIGURE 33. Convergence characteristics of optimization methods for annual energy loss minimization in Case 3 of 69-bus RDN.

harmony between exploration and exploitation. For the two WOA and SCA methods, they do not show the ability to efficiently explore the search space and suffer from a slow convergence speed when solving this case.

VI. CONCLUSION

In the paper, QOCNNA has been successfully proposed to solve the SNR-DG problem. Active power loss minimization and voltage stability index maximization in RDNs are the considered objective functions of the SNR-DG problem. The proposed QOCNNA is implemented to determine optimal configuration and positions and capacities of DGs for the 33-, 69-, and 118-bus RDNs at several scenarios with various case studies. For single-objective scenario, among three cases tested, the case of SNR-DG solved by QOCNNA is the most effective in reducing power loss in different load levels. Particularly, the PLRs at nominal load level after the SNR-DG by QOCNNA respectively are 73.01%, 84.28%, and 59.99% for the 33-, 69-, and 118-bus RDNs. Likewise, simulation results of multi-objective scenario also indicate that the optimal solution of SNR-DG found by QOCNNA leads to a significant improvement in network performance (i.e., power loss reduction and voltage stability index maximization) in all load conditions. Especially, as for case SNR-DG of the 33-, 69-, and 118-bus RDNs at nominal load condition, QOCNNA yields optimal solutions relative to PLR percentages of 70.79%, 84.02%, and 57.79%, respectively. At the same time, the OVSI improvement percentages are 16.36%, 8.59%, and 10.10%, respectively. The solutions offered by QOCNNA result in a better improvement in network performance than the ones found by NNA, ALO as well as previous methods in the literature in both scenarios. Further, QOCNNA shows a better convergence and lower standard deviation of solutions when compared with NNA and ALO for all case studies in two scenarios. Moreover, QOCNNA obtains the optimal network configuration and settings of PV DG satisfying the daily variable load demand and generation while minimizing total annual energy loss. The solution of QOCNNA in this scenario leads to more reduction in total annual energy loss than those of analytical-based approaches and other applied methods as well.

In conclusion, QOCNNA is capable of finding high-quality solutions with fast convergence speed and small standard deviation of solutions for the SNR-DG problem. In most cases, the optimized outcomes by QOCNNA are highly competitive and effective against the previous studies. This proves the improvement strategies help QOCNNA gain an excellent harmony between exploration and exploitation. For future researches, we will focus on expanding the SNR-DG problem as well as the QOCNNA algorithm in some aspects such as uncertainty in loads and renewable generations, combination of technical, economic, and reliability objectives, and development in the multi-objective version of QOCNNA. It is noted that the application of QOCNNA for handling the uncertainty issues relative to the SNR-DG problem is discussed as in Appendix B below.

APPENDIX

A. EXAMINATION OF DAILY LOAD AND GENERATION VARIATIONS ON NR AND DG ALLOCATION PROBLEM

The procedure for NR and PV DG allocation considering daily variable load and generation is presented as:

1. Read the predicted data relative to the 24-h load.
2. Perform a 24-h load flow and calculate the total annual energy loss for the initial case using Eq. (35).
3. Randomly initialize the opened switches, location and sizes of one PV DG for each case study using the equations (A.1 – A.3) in which the numbers of control variables are 5, 49 and 54 corresponding to the NR-only, PV DG-only and simultaneous NR – PV DG cases:

$$X_i = [S_1, \ldots, S_{N_{SW}}]; \quad i = 1, \ldots, N_P \tag{A.1}$$

$$X_i = [L, P_1, \ldots, P_h, Q_1, \ldots, Q_h]; \quad i = 1, \ldots, N_P; \quad h = 24 \tag{A.2}$$

$$X_i = [S_1, \ldots, S_{N_{SW}}, L, P_1, \ldots, P_h, Q_1, \ldots, Q_h]; \quad i = 1, \ldots, N_P; \quad h = 24 \tag{A.3}$$

where $P_1, \ldots, P_h$ and $Q_1, \ldots, Q_h$ are respectively active and reactive power outputs of PV DG for a 24-h period.

The control variables of S_i, L, P_t, Q_t are randomly initialized using the following equations:

$$S_i = round[S_{i,\min} + rand(0,1) \times (S_{i,\max} - S_{i,\min})], \quad i = 1, \ldots, N_{SW} \tag{A.4}$$

$$L = round[L_{\min} + rand(0,1) \times (L_{\max} - L_{\min})] \tag{A.5}$$

$$P_t = P_{t,\min} + rand(0,1) \times (P_{t,\max} - P_{t,\min}), \quad t = 1, \ldots, h \tag{A.6}$$

$$Q_t = Q_{t,\min} + rand(0,1) \times (Q_{t,\max} - Q_{t,\min}), \quad t = 1, \ldots, h \tag{A.7}$$

This study assumes that PV DG adopts advanced technologies (i.e., using converters for connection) allowing operation at a desired power factor. With the

non-dispatchable nature, the output of PV DG depends on the generation curve for 24-h a day as in [40]. Based on this generation curve, the hourly output is equivalent to a daily peak output percentage of the DG unit. Therefore, the output range of PV DG for optimization at the hour t will be from 0% to 100% of the output at the hour t of the DG unit. Also, the location of PV DG may be determined by geographic and resource factors. For a benchmark RDN, the nodes for DG allocation are not predetermined and so all nodes except slack node are considered as candidate nodes for DG placement. In other words, the search range for the PV DG placement will be from node 2 to node n.

4. Execute the QOBL process to create the population QOX. Evaluate the fitness function for all candidate solutions in X and QOX according to Eqs. (A.8) and (A.9). Choose N_P best solutions from $\{X, QOX\}$.

$$FF_{AEL} = AEL + \sum_{h=1}^{24} penal_h \tag{A.8}$$

where $penal_h$ is a penalty function for controlling the violation of related constraints in the hour h of the day and is formulated as follows:

$$penal_h = K \times \left(\sum_{i=1}^{N_B} (V_i^h - V_i^{\lim})^2 + \sum_{i=1}^{N_L} (I_k^h - I_k^{\lim})^2 + (PE_{DG} - PE_{DG}^{\lim,h})^2 \right) \tag{A.9}$$

where K is the penalty factor set to 10^3 for the investigations in this scenario and $PE_{DG}^{\lim,h}$ is the penetration limit of PV DG in the hour h depending on the total load demand of the network at that hour.

5. Define target items X_{Target} and W_{Target}.
6. Assign $t = 0$ and $\beta = 1$.
7. while $(t < T_{\max})$ do
8. Generate new solutions and update the solutions via Eqs. (17) and (18). Update W using Eq. (19).
9. If $rand \leq \beta$, execute the bias operator to update new solutions and weight matrix (Algorithm 1). Otherwise, apply the transfer function operator using Eq. (21) for solution update.
10. Update β using Eq. (20).
11. If $rand < j_r$, perform the QOBL method to acquire quasi-oppositional points of the current population. These new solutions are only updated if their fitness values are better.
12. Update X_{Target} and W_{Target}.
13. Implement the CLS strategy to find a better target solution;
14. $t = t + 1$
15. end while
16. Return optimal solution of the opened switches, location, outputs of PV DG in relation to practical 24-h load variations. After acquiring the optimal hourly outputs of PV DG, the apparent power and the optimal pf of PV DG at hour t can be respectively computed using Eqs. (A.10) and (A.11):

$$S_{DG,t} = \sqrt{P_{DG,t}^2 + Q_{DG,t}^2} \tag{A.10}$$

$$pf_{DG,t} = \frac{P_{DG,t}^2}{\sqrt{P_{DG,t}^2 + Q_{DG,t}^2}} \tag{A.11}$$

B. DISCUSSION ON THE APPLICATION OF QOCNNA FOR HANDLING THE UNCERTAINTY ISSUES OF THE PROBLEM

For the optimization problem of NR and DG allocation in RDNs, the load-predicting errors along with PV and wind power generation considered as some main sources of uncertainty can be included in the mathematical modelling. To deal with these uncertainty parameters, there are three main approach groups in the literature including probabilistic approaches, possibilistic approaches and hybrid probabilistic-possibilistic approaches [49]. In this section, we will present the application of a commonly used probabilistic strategy of Monte Carlo simulation (MCS) belonging to the probabilistic approaches group for handling relevant uncertainties. Regarding the application, uncertain parameters are first modelled by probability density functions (PDFs) and are then dealt with MCS strategy. Electrical loads, PV and wind power generation can be modelled by using the common PDFs as follows:

1) ELECTRICAL LOAD

Due to the errors in prediction, the loads are frequently modeled as a Gaussian PDF in which the mean of the PDF is equal to the predicted load value. In most cases, a division of predicted value is taken as the PDF's standard deviation [50], [51].

$$PDF(S_L) = \frac{1}{\sqrt{2\pi}\sigma} \exp\left[-\frac{(S_L - \mu)^2}{2\sigma^2} \right] \tag{B.1}$$

where S_L represents load's apparent power; σ and μ denote the mean and standard deviation of load power, respectively.

2) PV POWER GENERATION

The power generated by a PV DG is primarily related to solar irradiation [50], [52], [53]. Solar irradiation is frequently modeled as a Beta PDF characterized by the following equation [50].

$$PDF(s) = \begin{cases} \dfrac{\Gamma(\alpha+\beta)}{\Gamma(\alpha)\cdot\Gamma(\beta)} \cdot s^{\alpha-1} \cdot (1-s)^{\beta-1} & \text{if } 0 \leq s \leq 1 \\ x & \text{otherwise} \end{cases} \tag{B.2}$$

where s denotes solar irradiation (kW/m^2); α and β represent parameters relative to Beta distribution.

3) WIND POWER GENERATION

The power generated by a wind turbine is primarily related to the wind speed [50], [54], [55]. Wind speed is frequently characterized by Weibull distribution as follows [50], [56], [57].

$$PDF(v) = \left(\frac{k}{c}\right)\left(\frac{v}{c}\right)^{k-1} e^{\left(\frac{v}{c}\right)^k} \tag{B.3}$$

where k and c are shape and scale factors of Weibull function, respectively.

The power generated by a wind turbine follows a function of wind speed and is estimated using Eq. (B.4).

$$P(v) = \begin{cases} 0 & v < v_{in} \text{ or } v > v_{out} \\ \dfrac{v - v_{in}}{v_{rated} - v_{in}} & v_{in} \le v \le v_{rated} \\ P_{rated} & v_r < v \le v_{out} \end{cases} \tag{B.4}$$

where P_{rated} is wind turbine's rated power; v_{rated} is rated speed of turbine (m/s); v_{in} and v_{out} are cut-in speed and cut-out speed of wind turbine (m/s), respectively.

After describing the uncertain parameters of the problem by PDFs, the probabilistic uncertainty handling technique of MCS is adopted for computations. Specifically, the input-output relationship of the problem is represented as follows:

$$y = f(X, U) \tag{B.5}$$

where X denotes the set of uncertain input parameters, i.e., loads, generation power of PV DG and wind DG; U denotes the set of control variables, i.e., open switches and site of DGs and y denotes the objective function to be minimized of the problem.

More specifically, in this case, the opened switches and site of DGs will be found using the proposed QOCNNA so that the object function in Eq. (B.5) is minimized while considering the uncertainties of loads and generation power of PV and wind DGs. In the iteration process of MCS, for each pattern solution from population initialized by the QOCNNA, different samples of loads and generation power of PV and wind DGs are generated corresponding to each fixed value of U using PDFs, the respective values of object function are then estimated for each sample based on input-output relation. Afterwards, the mean of object function values is judged as the quality of that pattern solution. For this case, different pattern solutions are assessed at different iterations and the best pattern solution is chosen as the optimal solution when the stopping condition is achieved. Below is the pseudo-code of MCS for handling the uncertain parameters.

for $i = 1: n_{trial}$

Create sample X_i of loads and generation power of PV and wind DGs.

Compute $y_i = f(X_i, Z)$

end for

$$mean = \frac{\sum_{i=1}^{n_{trial}} y_i}{n_{trial}} \tag{B.6}$$

$$std = \sqrt{\frac{\sum_{i=1}^{n_{trial}} (y_i - mean)^2}{n_{trial}}} \tag{B.7}$$

where n_{trial} is the number of MCS trials; *mean* and *std* are the mean and standard deviation of the y's Gaussian PDF.

ACKNOLEDGMENT

The present research study was funded by Thu Dau Mot University (TDMU) under grant number DT.21.1-079.

REFERENCES

[1] A. Ameli, A. Ahmadifar, M.-H. Shariatkhah, and M. Vakilian, "A dynamic method for feeder reconfiguration and capacitor switching in smart distribution systems," *Int. J. Elect. Power Energy Syst.*, vol. 85, pp. 200–211, Feb. 2017, doi: 10.1016/j.ijepes.2016.09.008.

[2] A. Merlin, "Search for a minimal-loss operating spanning tree configuration for an urban power distribution system," in *Proc. Power Syst. Comput. Conf.*, vol. 1, 1975, pp. 1–18.

[3] S. Ghasemi and J. Moshtagh, "A novel codification and modified heuristic approaches for optimal reconfiguration of distribution networks considering losses cost and cost benefit from voltage profile improvement," *Appl. Soft Comput.*, vol. 25, pp. 360–368, Dec. 2014, doi: 10.1016/j.asoc.2014.08.068.

[4] D. Shirmohammadi and H. W. Hong, "Reconfiguration of electric distribution networks for resistive line losses reduction," *IEEE Trans. Power Syst.*, vol. 4, no. 1, pp. 1492–1498, Apr. 1989, doi: 10.1109/61.25637.

[5] A. Y. Abdelaziz, F. M. Mohammed, S. F. Mekhamer, and M. A. L. Badr, "Distribution systems reconfiguration using a modified particle swarm optimization algorithm," *Electr. Power Syst. Res.*, vol. 79, no. 11, pp. 1521–1530, Nov. 2009, doi: 10.1016/j.epsr.2009.05.004.

[6] A. M. Othman, A. A. El-Fergany, and A. Y. Abdelaziz, "Optimal reconfiguration comprising voltage stability aspect using enhanced binary particle swarm optimization algorithm," *Electr. Power Compon. Syst.*, vol. 43, no. 14, pp. 1656–1666, Aug. 2015, doi: 10.1080/15325008.2015.1041623.

[7] J. Z. Zhu, "Optimal reconfiguration of electrical distribution network using the refined genetic algorithm," *Electr. Power Syst. Res.*, vol. 62, no. 1, pp. 37–42, May 2002, doi: 10.1016/S0378-7796(02)00041-X.

[8] H. de Faria, M. G. Resende, and D. Ernst, "A biased random key genetic algorithm applied to the electric distribution network reconfiguration problem," *J. Heuristics*, vol. 23, no. 6, pp. 533–550, 2017, doi: 10.1007/s10732-017-9355-8.

[9] R. S. Rao, S. V. L. Narasimham, M. R. Raju, and A. S. Rao, "Optimal network reconfiguration of large-scale distribution system using harmony search algorithm," *IEEE Trans. Power Syst.*, vol. 26, no. 3, pp. 1080–1088, Aug. 2011, doi: 10.1109/TPWRS.2010.2076839.

[10] D. Das, "A fuzzy multiobjective approach for network reconfiguration of distribution systems," *IEEE Trans. Power Del.*, vol. 21, no. 1, pp. 202–209, Jan. 2006, doi: 10.1109/TPWRD.2005.852335.

[11] A. M. Imran and M. Kowsalya, "A new power system reconfiguration scheme for power loss minimization and voltage profile enhancement using fireworks algorithm," *Int. J. Elect. Power Energy Syst.*, vol. 62, pp. 312–322, Nov. 2014, doi: 10.1016/j.ijepes.2014.04.034.

[12] M. Abdelaziz, "Distribution network reconfiguration using a genetic algorithm with varying population size," *Electr. Power Syst. Res.*, vol. 142, pp. 9–11, Jan. 2017, doi: 10.1016/j.epsr.2016.08.026.

[13] T. T. Nguyen and A. V. Truong, "Distribution network reconfiguration for power loss minimization and voltage profile improvement using cuckoo search algorithm," *Int. J. Elect. Power Energy Syst.*, vol. 68, pp. 233–242, Jun. 2015, doi: 10.1016/j.ijepes.2014.12.075.

[14] K. Mahmoud and M. Lehtonen, "Comprehensive analytical expressions for assessing and maximizing technical benefits of photovoltaics to distribution systems," *IEEE Trans. Smart Grid*, vol. 12, no. 6, pp. 4938–4949, Nov. 2021, doi: 10.1109/TSG.2021.3097508.

[15] K. Mahmoud and M. Lehtonen, "Simultaneous allocation of multi-type distributed generations and capacitors using generic analytical expressions," *IEEE Access*, vol. 7, pp. 182701–182710, 2019, doi: 10.1109/ACCESS.2019.2960152.

[16] K. Mahmoud, N. Yorino, and A. Ahmed, "Optimal distributed generation allocation in distribution systems for loss minimization," *IEEE Trans. Power Syst.*, vol. 31, no. 2, pp. 960–969, Mar. 2016, doi: 10.1109/TPWRS.2015.2418333.

[17] A. M. Shaheen, A. M. Elsayed, R. A. El-Sehiemy, and A. Y. Abdelaziz, "Equilibrium optimization algorithm for network reconfiguration and distributed generation allocation in power systems," *Appl. Soft Comput.*, vol. 98, Jan. 2021, Art. no. 106867, doi: 10.1016/j.asoc.2020.106867.
[18] A. Onlam, D. Yodphet, R. Chatthaworn, C. Surawanitkun, A. Siritaratiwat, and P. Khunkitti, "Power loss minimization and voltage stability improvement in electrical distribution system via network reconfiguration and distributed generation placement using novel adaptive shuffled frogs leaping algorithm," *Energies*, vol. 12, no. 3, p. 553, Jan. 2019, doi: 10.3390/en12030553.
[19] V. V. V. S. N. Murty and A. Kumar, "Optimal DG integration and network reconfiguration in microgrid system with realistic time varying load model using hybrid optimisation," *IET Smart Grid*, vol. 2, no. 2, pp. 192–202, Jun. 2019, doi: 10.1049/iet-stg.2018.0146.
[20] H. B. Tolabi, M. H. Ali, S. B. M. Ayob, and M. Rizwan, "Novel hybrid fuzzy-bees algorithm for optimal feeder multi-objective reconfiguration by considering multiple-distributed generation," *Energy*, vol. 71, pp. 507–515, Jul. 2014, doi: 10.1016/j.energy.2014.04.099.
[21] K. Muthukumar and S. Jayalalitha, "Integrated approach of network reconfiguration with distributed generation and shunt capacitors placement for power loss minimization in radial distribution networks," *Appl. Soft Comput.*, vol. 52, pp. 1262–1284, Mar. 2017, doi: 10.1016/j.asoc.2016.07.031.
[22] R. Syahputra, I. Robandi, and M. Ashari, "Reconfiguration of distribution network with DG using fuzzy multi-objective method," in *Proc. Int. Conf. Innov. Manage. Technol. Res.*, May 2012, pp. 316–321, doi: 10.1109/ICIMTR.2012.6236410.
[23] R. Rajaram, K. S. Kumar, and N. Rajasekar, "Power system reconfiguration in a radial distribution network for reducing losses and to improve voltage profile using modified plant growth simulation algorithm with distributed generation (DG)," *Energy Rep.*, vol. 1, pp. 116–122, Nov. 2015, doi: 10.1016/j.egyr.2015.03.002.
[24] A. Bayat, A. Bagheri, and R. Noroozian, "Optimal siting and sizing of distributed generation accompanied by reconfiguration of distribution networks for maximum loss reduction by using a new UVDA-based heuristic method," *Int. J. Electr. Power Energy Syst.*, vol. 77, pp. 360–371, May 2016, doi: 10.1016/j.ijepes.2015.11.039.
[25] U. Raut and S. Mishra, "An improved sine–cosine algorithm for simultaneous network reconfiguration and DG allocation in power distribution systems," *Appl. Soft Comput.*, vol. 92, Jul. 2020, Art. no. 106293, doi: 10.1016/j.asoc.2020.106293.
[26] R. S. Rao, K. Ravindra, K. Satish, and S. V. L. Narasimham, "Power loss minimization in distribution system using network reconfiguration in the presence of distributed generation," *IEEE Trans. Power Syst.*, vol. 28, no. 1, pp. 317–325, Feb. 2013, doi: 10.1109/TPWRS.2012.2197227.
[27] T. T. Nguyen, A. V. Truong, and T. A. Phung, "A novel method based on adaptive cuckoo search for optimal network reconfiguration and distributed generation allocation in distribution network," *Int. J. Elect. Power Energy Syst.*, vol. 78, pp. 801–815, Jun. 2016, doi: 10.1016/j.ijepes.2015.12.030.
[28] A. M. Imran, M. Kowsalya, and D. P. Kothari, "A novel integration technique for optimal network reconfiguration and distributed generation placement in power distribution networks," *Int. J. Elect. Power Energy Syst.*, vol. 63, pp. 461–472, Dec. 2014, doi: 10.1016/j.ijepes.2014.06.011.
[29] M. Esmaeili, M. Sedighizadeh, and M. Esmaili, "Multi-objective optimal reconfiguration and DG (distributed generation) power allocation in distribution networks using big bang-big crunch algorithm considering load uncertainty," *Energy*, vol. 103, pp. 86–99, May 2016, doi: 10.1016/j.energy.2016.02.152.
[30] M. Sedighizadeh, M. Esmaili, and M. Esmaeili, "Application of the hybrid big bang-big crunch algorithm to optimal reconfiguration and distributed generation power allocation in distribution systems," *Energy*, vol. 76, pp. 920–930, Nov. 2014, doi: 10.1016/j.energy.2014.09.004.
[31] M. Abd El-Salam, E. Beshr, and M. Eteiba, "A new hybrid technique for minimizing power losses in a distribution system by optimal sizing and siting of distributed generators with network reconfiguration," *Energies*, vol. 11, no. 12, p. 3351, Nov. 2018, doi: 10.3390/en11123351.
[32] Z. Gong, Q. Chen, and K. Sun, "Novel methodology solving distribution network reconfiguration with DG placement," *J. Eng.*, vol. 2019, no. 16, pp. 1668–1674, Mar. 2019, doi: 10.1049/joe.2018.8521.
[33] O. Badran, H. Mokhlis, S. Mekhilef, W. Dahalan, and J. Jallad, "Minimum switching losses for solving distribution NR problem with distributed generation," *IET Gener., Transmiss. Distrib.*, vol. 12, no. 8, pp. 1790–1801, Apr. 2018, doi: 10.1049/iet-gtd.2017.0595.
[34] H. Teimourzadeh and B. Mohammadi-Ivatloo, "A three-dimensional group search optimization approach for simultaneous planning of distributed generation units and distribution network reconfiguration," *Appl. Soft Comput.*, vol. 88, Mar. 2020, Art. no. 106012, doi: 10.1016/j.asoc.2019.106012.
[35] D. H. Wolper and W. G. Macready, "No free lunch theorems for optimization," *IEEE Trans. Evol. Comput.*, vol. 1, no. 1, pp. 67–82, Apr. 1997, doi: 10.1109/4235.585893.
[36] A. Sadollah, H. Sayyaadi, and A. Yadav, "A dynamic Metaheuristic optimization model inspired by biological nervous systems: Neural network algorithm," *Appl. Soft Comput.*, vol. 71, pp. 747–782, Oct. 2018, doi: 10.1016/j.asoc.2018.07.039.
[37] S. Mirjalili, "The ant lion optimizer," *Adv. Eng. Softw.*, vol. 83, pp. 80–98, May 2015, doi: 10.1016/j.advengsoft.2015.01.010.
[38] S. Mirjalili and A. Lewis, "The whale optimization algorithm," *Adv. Eng. Softw.*, vol. 95, pp. 51–67, Feb. 2016, doi: 10.1016/j.advengsoft.2016.01.008.
[39] S. Mirjalili, "SCA: A sine cosine algorithm for solving optimization problems," *Knowl.-Based Syst.*, vol. 96, pp. 120–133, Mar. 2016, doi: 10.1016/j.knosys.2015.12.022.
[40] D. Q. Hung, N. Mithulananthan, and R. C. Bansal, "Analytical strategies for renewable distributed generation integration considering energy loss minimization," *Appl. Energy*, vol. 105, pp. 75–85, May 2013, doi: 10.1016/j.apenergy.2012.12.023.
[41] A. Y. Abdelaziz, F. M. Mohamed, S. F. Mekhamer, and M. A. L. Badr, "Distribution system reconfiguration using a modified tabu search algorithm," *Electr. Power Syst. Res.*, vol. 80, no. 8, pp. 943–953, Aug. 2010, doi: 10.1016/j.epsr.2010.01.001.
[42] H. R. Tizhoosh, "Opposition-based learning: A new scheme for machine intelligence," in *Proc. Int. Conf. Comput. Intell. Modeling, Control Autom. Int. Conf. Intell. Agents, Web Technol. Internet Commerce (CIMCA-IAWTIC06)*, Nov. 2005, pp. 695–701, doi: 10.1109/CIMCA.2005.1631345.
[43] S. Rahnamayan, H. R. Tizhoosh, and M. M. A. Salama, "Quasi-oppositional differential evolution," in *Proc. IEEE Congr. Evol. Comput.*, Sep. 2007, pp. 2229–2236, doi: 10.1109/CEC.2007.4424748.
[44] D. Jia, G. Zheng, and M. K. Khan, "An effective memetic differential evolution algorithm based on chaotic local search," *Inf. Sci.*, vol. 181, no. 15, pp. 3175–3187, Aug. 2011, doi: 10.1016/j.ins.2011.03.018.
[45] J. Ji, S. Gao, S. Wang, Y. Tang, H. Yu, and Y. Todo, "Self-adaptive gravitational search algorithm with a modified chaotic local search," *IEEE Access*, vol. 5, pp. 17881–17895, 2017, doi: 10.1109/ACCESS.2017.2748957.
[46] R. D. Zimmerman and C. E. Murillo-Sanchez. (2011). MATPOWER-Manual-4.1.pdf. Power Systems Engineering Research Center. Cornell University. Ithaca, NY, USA. Accessed: Sep. 19, 2020. [Online]. Available: https://matpower.org/docs/MATPOWER-manual-4.1.pdf
[47] M. E. Baran and F. F. Wu, "Network reconfiguration in distribution systems for loss reduction and load balancing," *IEEE Trans. Power Del.*, vol. 4, no. 2, pp. 1401–1407, Apr. 1989, doi: 10.1109/61.25627.
[48] M. E. Baran and F. F. Wu, "Optimal capacitor placement on radial distribution systems," *IEEE Trans. Power Del.*, vol. 4, no. 1, pp. 725–734, Jan. 1989, doi: 10.1109/61.19265.
[49] A. Soroudi and T. Amraee, "Decision making under uncertainty in energy systems: State of the art," *Renew. Sustain. Energy Rev.*, vol. 28, pp. 376–384, Dec. 2013, doi: 10.1016/j.rser.2013.08.039.
[50] A. Soroudi, M. Aien, and M. Ehsan, "A probabilistic modeling of photo voltaic modules and wind power generation impact on distribution networks," *IEEE Syst. J.*, vol. 6, no. 2, pp. 254–259, Jun. 2012, doi: 10.1109/JSYST.2011.2162994.
[51] F. Liu, Z. Bie, S. Liu, and T. Ding, "Day-ahead optimal dispatch for wind integrated power system considering zonal reserve requirements," *Appl. Energy*, vol. 188, pp. 399–408, Feb. 2017, doi: 10.1016/j.apenergy.2016.11.102.
[52] M. N. Kabir, Y. Mishra, and R. C. Bansal, "Probabilistic load flow for distribution systems with uncertain PV generation," *Appl. Energy*, vol. 163, pp. 343–351, Feb. 2016, doi: 10.1016/j.apenergy.2015.11.003.
[53] B. R. Prusty and D. Jena, "A critical review on probabilistic load flow studies in uncertainty constrained power systems with photovoltaic generation and a new approach," *Renew. Sustain. Energy Rev.*, vol. 69, pp. 1286–1302, Mar. 2017, doi: 10.1016/j.rser.2016.12.044.

[54] G. Aquila, P. Rotela, Jr., E. de Oliveira Pamplona, and A. R. de Queiroz, "Wind power feasibility analysis under uncertainty in the Brazilian electricity market," *Energy Econ.*, vol. 65, pp. 127–136, Jun. 2017, doi: 10.1016/j.eneco.2017.04.027.

[55] P. Xiong, P. Jirutitijaroen, and C. Singh, "A distributionally robust optimization model for unit commitment considering uncertain wind power generation," *IEEE Trans. Power Syst.*, vol. 32, no. 1, pp. 39–49, Jan. 2017, doi: 10.1109/TPWRS.2016.2544795.

[56] S. Karaki, R. B. Chedid, and R. Ramadan, "Probabilistic performance assessment of autonomous solar-wind energy conversion systems," *IEEE Trans. Energy Convers.*, vol. 14, no. 3, pp. 766–772, Sep. 1999, doi: 10.1109/60.790949.

[57] J. Zhou, P. Lu, Y. Li, C. Wang, L. Yuan, and L. Mo, "Short-term hydro-thermal-wind complementary scheduling considering uncertainty of wind power using an enhanced multi-objective bee colony optimization algorithm," *Energy Convers. Manage.*, vol. 123, pp. 116–129, Sep. 2016, doi: 10.1016/j.enconman.2016.05.073.

THANH VAN TRAN received the B.Eng., M.Eng., and D.Eng. degrees in electrical engineering from Kyiv Polytechnic Institute, Kyiv, Ukraine, in 1992, 1994, and 2000, respectively. He is currently a Senior Lecturer with the Institute of Engineering and Technology, Thu Dau Mot University, Binh Duong, Vietnam. His research interests include applications of AI in power system optimization, power system operation and control, and power system analysis.

BAO-HUY TRUONG received the B.Eng. degree in electrical and electronics engineering from the Ho Chi Minh City University of Technology (HCMUT), VNU-HCM, Vietnam, in 2017, and the M.S. degree in electrical and electronics engineering from Universiti Teknologi PETRONAS (UTP), Malaysia, in 2020. He is currently a Research Officer with the Institute of Engineering and Technology, Thu Dau Mot University, Binh Duong, Vietnam. His research interests include renewable energy power generation, and artificial intelligence-based algorithms and their application in optimization problems.

TRI PHUOC NGUYEN received the B.Eng. degree in electrical engineering from Can Tho University, Can Tho, Vietnam, in 2014, and the M.Eng. degree in electrical engineering from the Ho Chi Minh City University of Technology, Ho Chi Minh City, Vietnam, in 2017. His research interest includes development and application of optimization algorithms to optimization of power systems.

THI ANH NGUYEN received the bachelor's degree in pharmacy from the Can Tho University of Medicine and Pharmacy, Vietnam, in 2017, and the master's degree in clinical pharmacology from Toulouse III Paul Sabatier University, France, in 2019. Her research interest includes applying optimization algorithms for multi-disciplinary problems in real-world setting. Besides, she is also interested in promoting the safe and effective use of drugs using modeling and simulation techniques.

THANH LONG DUONG received the B.Eng. and M.Eng. degrees in electrical engineering from the University of Technical Education Ho Chi Minh City, Vietnam, in 2003 and 2005, respectively, and the Ph.D. degree in electrical engineering from Hunan University, China, in 2014. He currently works with the Faculty of Electrical Engineering Technology, Industrial University of Ho Chi Minh City, Ho Chi Minh City, Vietnam. His research interests include power system operation, power system optimization, FACTS, renewable energy, optimization algorithm, and power markets.

DIEU NGOC VO received the B.Eng. and M.Eng. degrees in electrical engineering from the Ho Chi Minh City University of Technology (HCMUT), VNU-HCM, Ho Chi Minh City, Vietnam, in 1995 and 2000, respectively, and the D.Eng. degree in energy from the Asian Institute of Technology (AIT), Pathum Thani, Thailand, in 2007. He is currently an Associate Professor with the Department of Power Systems, Faculty of Electrical and Electronic Engineering, HCMUT. His research interests include applications of AI in power system optimization, power system operation and control, power system analysis, and power systems under deregulation.